LEHIGH UNIVERSITY

ME 454

Analysis of F-22 Raptor

Report by

Jayadeep Reddy Tangirala

Under the guidance of

Prof. Terry Hart

Project Outline

Project Objective: Analysis and Control System Design for the F-22 Raptor

Introduction

In the realm of aerospace engineering, the integration of advanced control systems into aircraft design is paramount for enhancing performance, stability, and safety. The F-22 Raptor, a pinnacle of modern air superiority featuring stealth, supercruise, advanced avionics, and highly integrated computer systems, presents an intriguing subject for such an analysis. This project, conducted as part of ME 454 Automatic Control of Aerospace Vehicles at Lehigh University, aims to delve into the aerodynamic properties and control system design of the F-22 Raptor.

Project Goals

The primary objective of this project is to analyze the F-22 Raptor's dynamic behaviour under various flight conditions and subsequently design appropriate control systems to improve its stability and handling characteristics. The project is divided into three main reports, each focusing on different aspects of aircraft control theory and application:

1. Aerodynamic Analysis and Stability Derivative Estimation:
   - <u>Objective</u>: Utilize available data on the physical dimensions, weight, and mass properties of the F-22 Raptor to estimate its stability derivatives using techniques from academic literature and aerospace software tools. Assumptions based on similar high-performance aircraft will be critical in estimating derivatives that are not directly calculable from available data.
   - <u>Deliverables</u>: Longitudinal and lateral state space models of the aircraft. Response plots for specific control inputs, namely a 2-second elevator doublet and a 1-second aileron input, will provide insights into the aircraft's responsiveness and stability characteristics under sudden manoeuvres.

2. Control System Design for Damping Enhancement:
   - <u>Objective</u>: Design and simulate pitch and yaw dampers to enhance the damping of the short-period pitch mode and the Dutch roll mode, respectively. This involves tweaking the control algorithms to fine-tune the aircraft's response to perturbations in these modes.
   - <u>Deliverables</u>: Simulations demonstrating the effectiveness of the dampers in improving aircraft stability and response characteristics. This report will also include the definition and analysis of one bending mode along the longitudinal axis and the corresponding aeroelastic stability derivatives.

3. Autopilot Design for Altitude and Heading Control:
   - <u>Objective:</u> Develop and simulate autopilot systems capable of maintaining a set altitude and heading. This involves creating robust control systems that can handle a step change of 100 feet in altitude and 3 degrees in heading, showcasing the autopilot's performance under typical operational scenarios.
   - <u>Deliverables</u>: Simulation results and analysis of the autopilot systems' dynamics, focusing on performance metrics such as overshoot, settling time, and steady-state error. We will extend this to include a damper design using the elevator to reduce vibrations in the defined longitudinal bending mode.

Methodology

The project will employ a combination of theoretical aerospace dynamics, computational simulations using MATLAB, XFLR5 and control system design principles. The initial phase will focus on gathering and synthesizing data on the F-22 Raptor's aerodynamic properties.

Subsequent phases will involve iterative design and simulation of control systems, with adjustments based on simulation outcomes.

Expected Outcomes
By the end of this project, we anticipate a comprehensive understanding of the F-22 Raptor's aerodynamic behaviour and control dynamics. The designed control systems are expected to demonstrate significant improvements in aircraft stability and response, potentially contributing to enhanced operational capabilities and safety measures. The project will culminate in detailed reports documenting the methodologies, analyses, and outcomes, supplemented by MATLAB codes and plots illustrating the work performed.

Conclusion
This project stands at the intersection of theoretical knowledge and practical application, aiming to bridge the gap between aerospace control theory and its implementation in one of the most advanced fighter jets in existence. Through rigorous analysis and innovative control design, this project will endeavour to push the boundaries of current aerospace control capabilities.

Report - 1

The primary goal of the first report in the series on the F-22 Raptor is to perform a detailed aerodynamic analysis using the aircraft's physical characteristics, such as dimensions, weight, and mass properties. By leveraging theoretical frameworks and aerospace software tools, stability derivatives will be estimated to reflect the unique flight dynamics of the F-22. This process will involve a comparative analysis with similar advanced fighter jets to validate the assumptions and enhance the accuracy of these derivatives. The stability derivatives derived from this analysis will then be used to construct comprehensive longitudinal and lateral state space models of the aircraft. These models are intended to accurately represent the Raptor's behaviour under normal and extreme operating conditions and will serve as the foundation for subsequent control system designs and simulations.

Following the development of these models, the report will focus on simulating the F-22 Raptor's response to specific control inputs, including a 2-second elevator doublet and a 1-second aileron input. These simulations will help assess the aircraft's stability and control effectiveness, particularly in response to rapid manoeuvres that are critical in combat scenarios. The outcomes of these simulations will be meticulously analyzed to identify any potential dynamic issues and to evaluate the overall performance of the aircraft under simulated conditions. This analysis will not only highlight the dynamic capabilities and limitations of the F-22 Raptor but also lay the groundwork for enhancing its control systems in future reports. The methodologies used, along with detailed MATLAB scripts and the results from the simulations, will be documented thoroughly, providing a valuable academic resource and a practical guide for further research and development in aerospace control applications.

The Geometry and Schematics of the F-22 Raptor

44' 6"

16' 5"

62' 1"
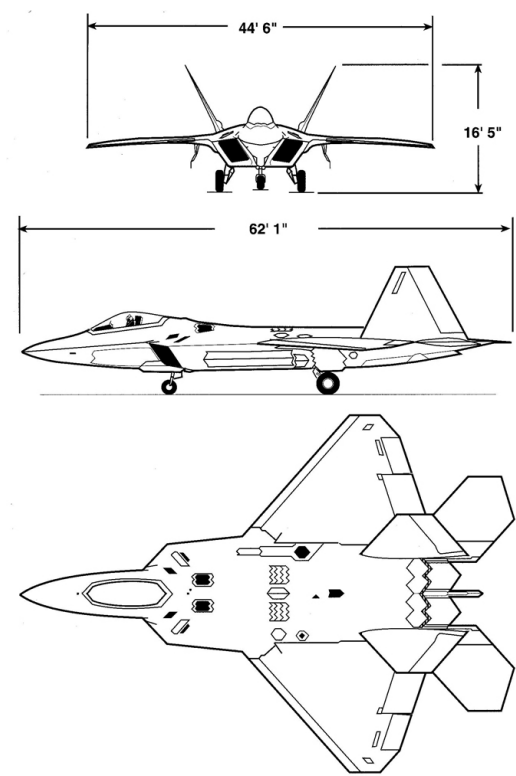
Aircraft Specifications

Length	62 ft / 18.90 m
Height	16.67 ft / 5.08 m
Wingspan	44.5 ft / 13.56 m
Wing Area	840 ft2 / 78.04 m2
Horizontal Tail Span	29 ft / 8.84 m
Engine Thrust Class	35,000 lb / 15,876 kg

Source: Official Lockheed Martin Website

General characteristics

- **Crew:** 1
- **Length:** 62 ft 1 in (18.92 m)
- **Wingspan:** 44 ft 6 in (13.56 m)
- **Height:** 16 ft 8 in (5.08 m)
- **Wing area:** 840 sq ft (78.04 m^2)
- **Aspect ratio:** 2.36
- **Airfoil:** NACA 6 series airfoil
- **Empty weight:** 43,340 lb (19,700 kg)
- **Gross weight:** 64,840 lb (29,410 kg)
- **Max takeoff weight:** 83,500 lb (38,000 kg)
- **Fuel capacity:** 18,000 lb (8,200 kg) internally, or 26,000 lb (12,000 kg) with two 2× 600 US gal tanks
- **Powerplant:** 2 × Pratt & Whitney F119-PW-100 augmented turbofans, 26,000 lbf (116 kN) thrust each dry, 35,000 lbf (156 kN) with afterburner[N 16]

Performance

- **Maximum speed:** Mach 2.25, 1,500 mph (2,414 km/h) at high altitude[121]
  - Mach 1.21, 800 knots (921 mph; 1,482 km/h) at sea level
- **Supercruise:** Mach 1.82, 1,220 mph (1,963 km/h) at high altitude
- **Range:** 1,600 nmi (1,800 mi, 3,000 km) or more with 2 external fuel tanks
- **Combat range:** 460 nmi (530 mi, 850 km) clean with 100 nmi (115 mi; 185 km) in supercruise
  - 590 nmi (679 mi; 1,093 km) clean subsonic[N 17]
- **Ferry range:** 1,740 nmi (2,000 mi, 3,220 km)
- **Service ceiling:** 65,000 ft (20,000 m)
- **g limits:** +9.0/−3.0
- **Wing loading:** 77.2 lb/sq ft (377 kg/m^2)
- **Thrust/weight:** 1.08 (1.25 with loaded weight and 50% internal fuel)

Source: Wikipedia Data

Dimensions

Geometric Characteristics	AR	Cr (ft)	Ct (ft)	S (ft^2)	ΛLE (deg)	Λ1/4 (deg)	λ	b (ft)
Wing	2.4	32.32	3.74	824.36	42	62.02	0.116	44.5
Horizontal Tail	6.18	9.35	3.74	136	42	47.94	0.4	29
Vertical Tail	1.94	17.53	4.2075	178	22.9	53.88	0.24	9.59

General dimensions										
WING										
wing span	AR	Wing Root chord	Wing tip chord	_LE	_TE	taper ratio	Anhedral	root twist	tip twist	t/c tip	t/c root
13.56m	2.4	9.85m	1.14m	42°	-17°	0.169	3.25°	5°	-3.1°	5.92%	4.29%

OVERALL								
length	height	wheelbase	weapons bay ground Clearance	weight (empty)	max T/O weight	W/S	T/W	
18.92m	5.08m	6.04m	.94m	14365 kg	27216 kg	348.7 kg/m^2	1.4	

- I tried to model the F-22 Raptor using AVL but it proved to be very complex Geometry to be modeled by AVL.
- Instead, I used XFLR5 Software which is X-Foil-based software with a Graphical User Interface.
- The AVL script for the flight is given in Appendix A of this Report

Airfoil Selection

- I used NACA 2412 Airfoil as I am analyzing only at subsonic speeds.
- Following is the Schematic of the Airfoil shape and the data of airfoils with flaps for the Main wing, Elevator and Fin
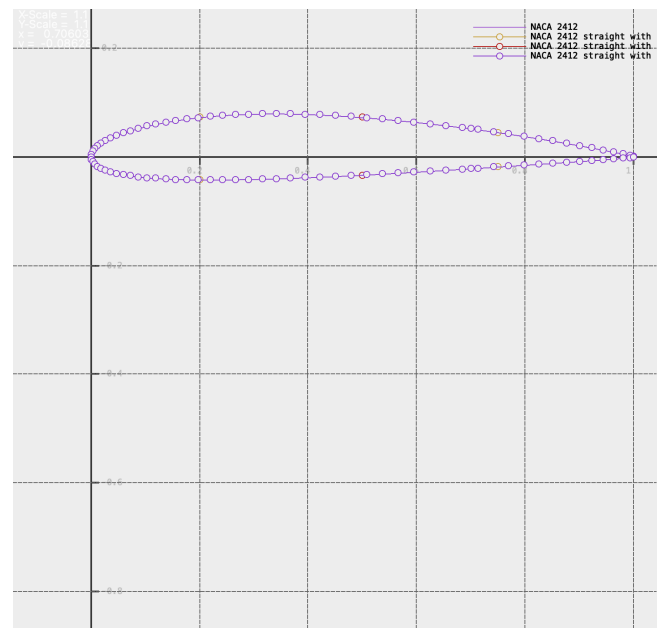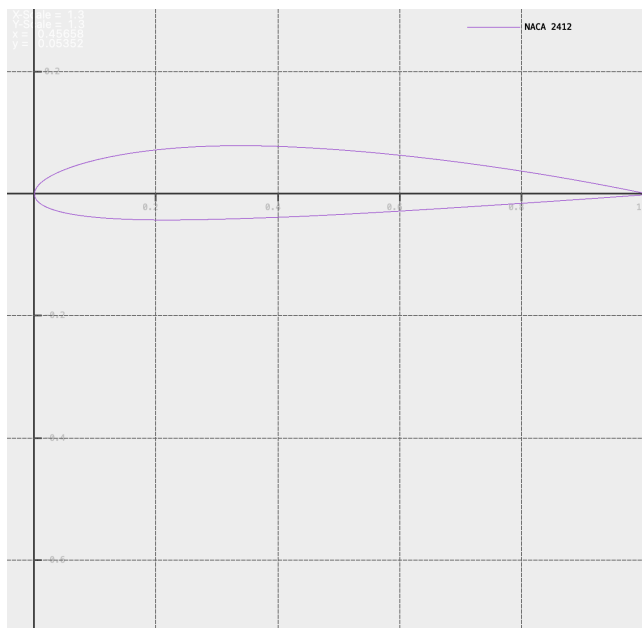
	Name	Thickness (%)	at (%)	Camber (%)	at (%)	Points	TE Flap (°)	TE XHinge	TE YHinge
1	Spline Foil	9.04	29.40	0.00	0.00	158	0.00	0.00	0.00
2	NACA 2412	12.00	29.03	2.00	39.54	99	0.00	0.00	0.00
3	NACA 2412 straight with Flaps	12.00	29.03	2.00	39.54	103	0.00	75.00	50.00
4	NACA 2412 straight with Flaps Elevator	12.00	29.03	2.00	39.54	101	0.00	50.00	50.00
5	NACA 2412 straight with Flaps Fin	12.00	29.03	2.00	39.54	101	0.00	70.00	50.00

AirFoil Analysis

- Now that we have an airfoil, We should Analyse the Airfoil.
- I am Using XFLR5 'Direct Foil Analysis Module' to analyse the Airfoil
- I analyzed Airfoil data for all the airfoil configurations for Multiple Reynolds Numbers and angles of attack configurations.
- The Angle of attack range was chosen from -10 degrees to +10 degrees with a step of half a degree change in the angle of attack.
- The Reynolds Number was analyzed to the range from 30000 to 49,152,000,000 which is quite a large range to ensure that analysis doesn't fall outside the Flight Envelope.
- For the above parameters, I ran Type1,2,3 and 4 analyses.
- This Analysis Generated around 320 plus polar data, of Which I will add a few in Appendix B.
- Below is the Screenshot of the Analysis
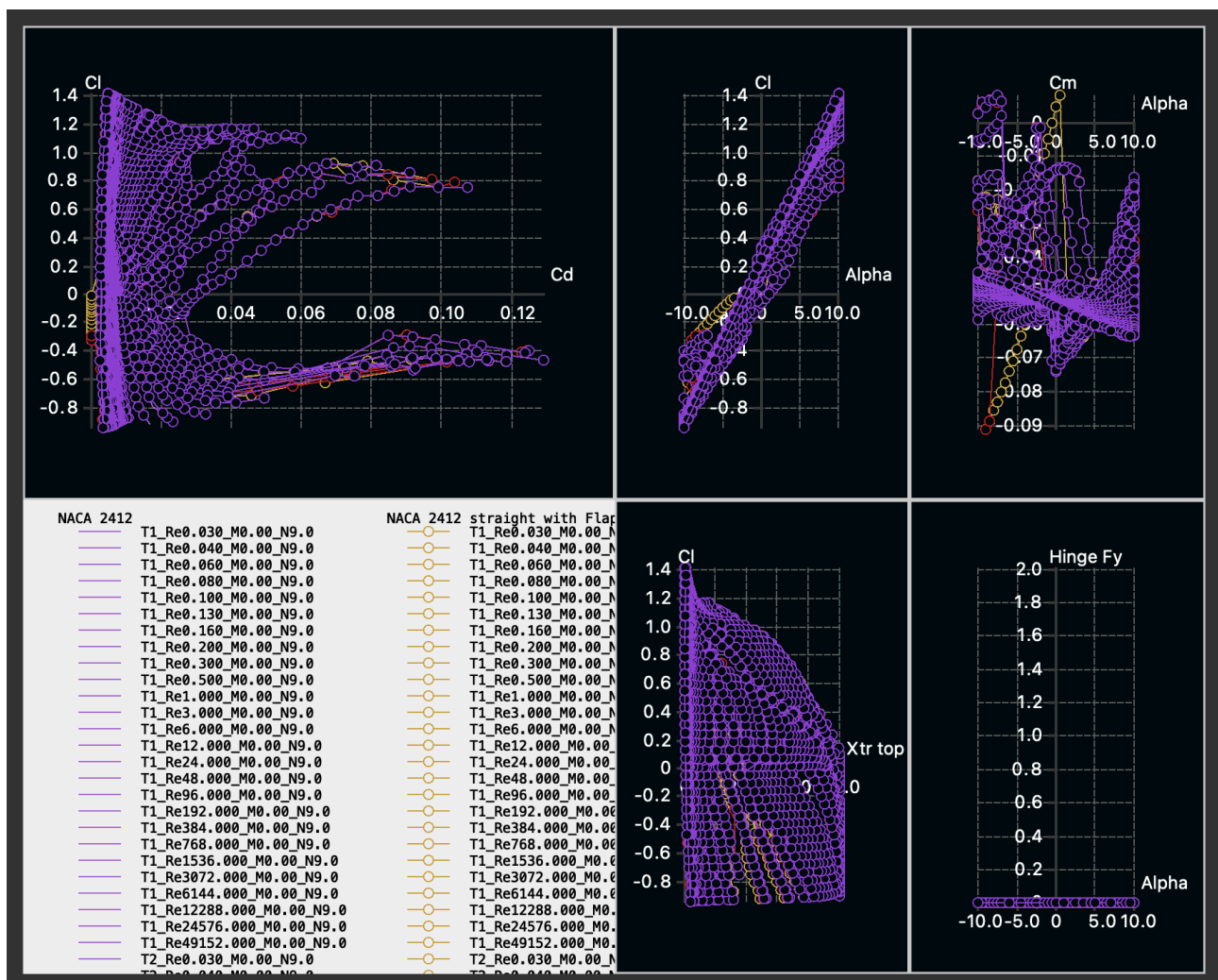
The Geometry

The Geometry is Mainly divided into three parts,

1) Main Wing
2) Elevator
3) Fin

Main Wing

- Below is a Screenshot from XFLR5 outlining the Key characteristics of the Main Wing

Wing Span	13.30	m
Area	66.12	m²
Projected Span	13.30	m
Projected Area	66.12	m²
Mean Geom.Chord	4.97	m
Mean Aero Chord	5.57	m
Aspect ratio	2.68	
Taper Ratio	0.15	
Root to Tip Sweep	32.74	°
Number of Flaps	0	
Number of VLM Panels	242	
Number of 3D Panels	506	

- The Dimensions of the main wing are as follows

Main Wing

☑ Symetric   ● Right Side   ○ Left Side   [Insert before section 1]   [Insert after section 1]   [Delete section 1]

	y ()	chord ()	offset ()	dihedral(°)	twist(°)	foil	X-panels	X-dist	Y-panels	Y-dist
1	0.000	7.600	0.000	0.0	5.00	NACA 2412		11 Cosine	3 Uniform	
2	0.000	7.600	0.000	0.0	5.00	NACA 2412		11 Cosine	2 Uniform	
3	2.090	5.700	1.900	0.0	5.00	NACA 2412		11 Cosine	2 Uniform	
4	2.090	5.700	1.900	0.0	5.00	NACA 2412 straight with I		11 Cosine	2 Uniform	
5	2.945	6.175	2.650	0.0	5.00	NACA 2412 straight with I		11 Cosine	2 Uniform	
6	2.945	6.175	2.650	0.0	5.00	NACA 2412 straight with I		11 Cosine	2 Uniform	
7	4.370	4.370	3.895	0.0	5.00	NACA 2412 straight with I		11 Cosine	2 Uniform	
8	4.370	4.370	3.895	0.0	5.00	NACA 2412 straight with I		11 Cosine	2 Uniform	
9	5.890	2.470	5.250	0.0	5.00	NACA 2412 straight with I		11 Cosine	3 Uniform	
10	5.890	2.470	5.250	0.0	5.00	NACA 2412 straight with I		11 Cosine	3 Uniform	
11	6.650	1.140	5.890	0.0	5.00	NACA 2412 straight with I		13 Cosine	2 Uniform	
12	6.650	1.140	5.890		5.00	NACA 2412				

- Below is a Screenshot from XFLR5 outlining the Key characteristics of the Elevator.

Wing Span	8.74	m
Area	21.98	m²
Projected Span	8.74	m
Projected Area	21.98	m²
Mean Geom.Chord	2.51	m
Mean Aero Chord	2.66	m
Aspect ratio	3.48	
Taper Ratio	0.64	
Root to Tip Sweep	29.48	°
Number of Flaps	0	
Number of VLM Panels	296	
Number of 3D Panels	606	

- The Dimensions of the Elevator are as follows,

Elevator

☑ Symetric   ⦿ Right Side   ◯ Left Side | Insert before section 1 | Insert after section 1 | Delete section 1 |

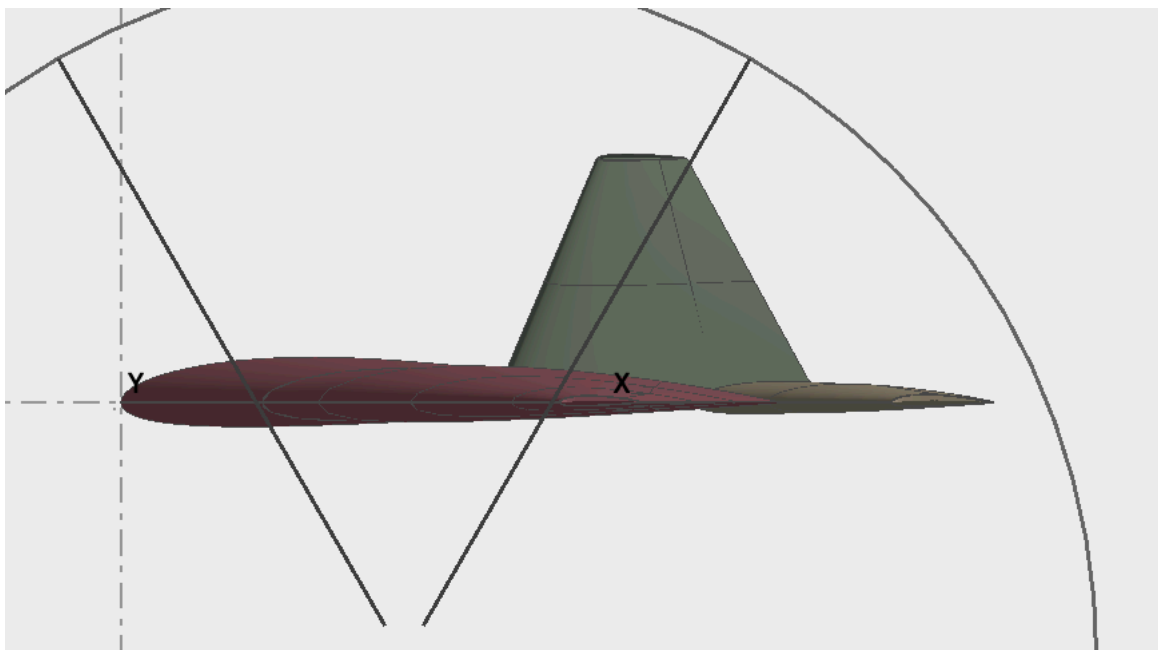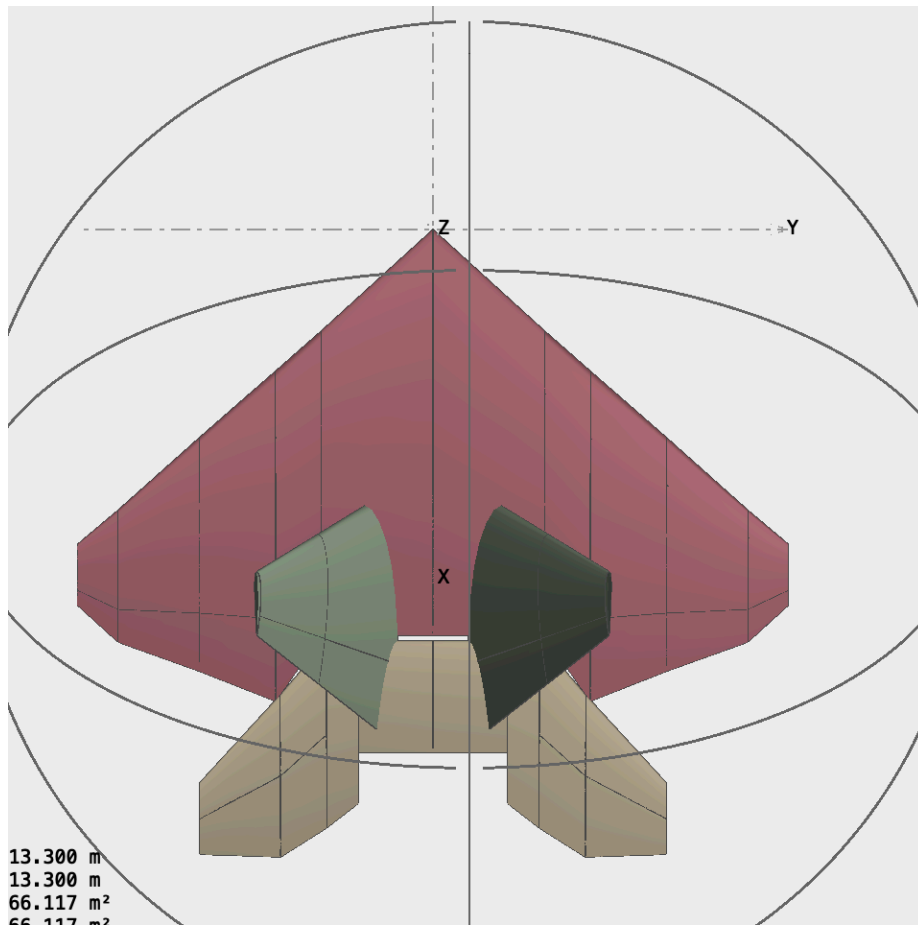|	y ()	chord ()	offset ()	dihedral(°)	twist(°)	foil	X-panels	X-dist	Y-panels	Y-dist
1	0.000	2.090	0.000	0.0	0.00	NACA 2412	7		10	Uniform
2	1.400	2.090	0.000	0.0	0.00	NACA 2412	7		9	Uniform
3	1.400	3.040	0.000	0.0	0.00	NACA 2412	13	Cosine	2	Uniform
4	1.995	3.500	0.000	0.0	0.00	NACA 2412	13	Cosine	2	Uniform
5	1.995	3.500	0.000	0.0	0.00	NACA 2412 straight with	13	Cosine	2	Uniform
6	2.850	3.040	1.000	0.0	0.00	NACA 2412 straight with	13	Cosine	2	Uniform
7	4.370	1.330	2.660		0.00	NACA 2412 straight with				

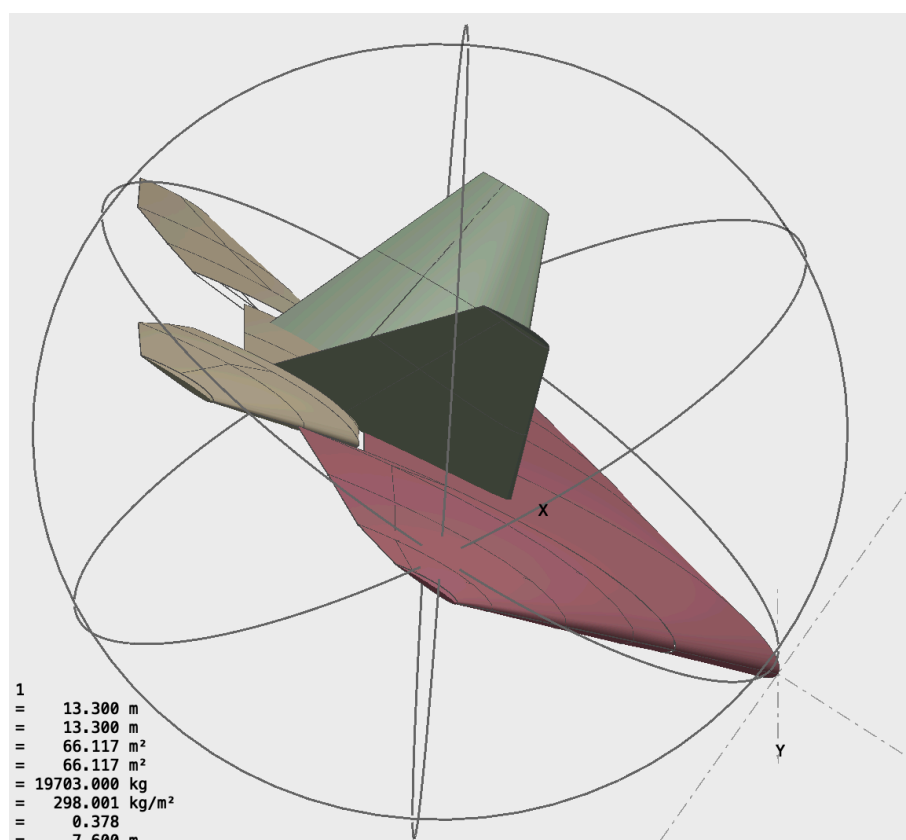- Below is a Screenshot from XFLR5 outlining the Key characteristics of the Fin.

Wing Span	8.00	m
Area	22.40	m²
Projected Span	6.55	m
Projected Area	18.35	m²
Mean Geom.Chord	2.80	m
Mean Aero Chord	3.10	m
Aspect ratio	2.86	
Taper Ratio	0.27	
Root to Tip Sweep	8.53	°
Number of Flaps	0	
Number of VLM Panels	70	
Number of 3D Panels	154	

- The Dimensions of the Fin are as follows,

Fin

☑ Symetric   ⦿ Right Side   ○ Left Side   [Insert before section 1]   [Insert after section 1]   [Delete section 1]

	y ()	chord ()	offset ()	dihedral(°)	twist(°)	foil	X-panels	X-dist	Y-panels	Y-dist
1	0.000	4.400	0.000	−35.0	0.00	NACA 2412 straight with	7	Uniform	5	Cosine
2	2.000	2.800	0.700	−35.0	0.00	NACA 2412 straight with	7	Uniform	5	Cosine
3	4.000	1.200	1.400		0.00	NACA 2412 straight with				

- The Final Geometry of the whole Plane without Fuesalage' is as follows


```
13.300 m
13.300 m
66.117 m²
66.117 m²
```

1
=   13.300 m
=   13.300 m
=   66.117 m²
=   66.117 m²
= 19703.000 kg
=   298.001 kg/m²
=   0.378
=   7.600 m
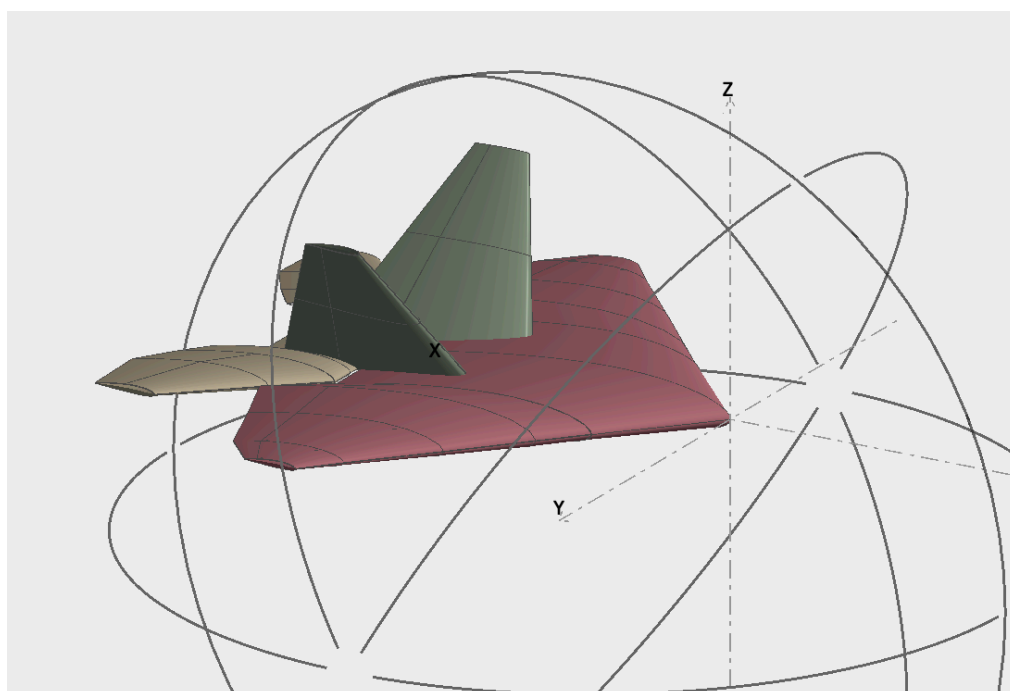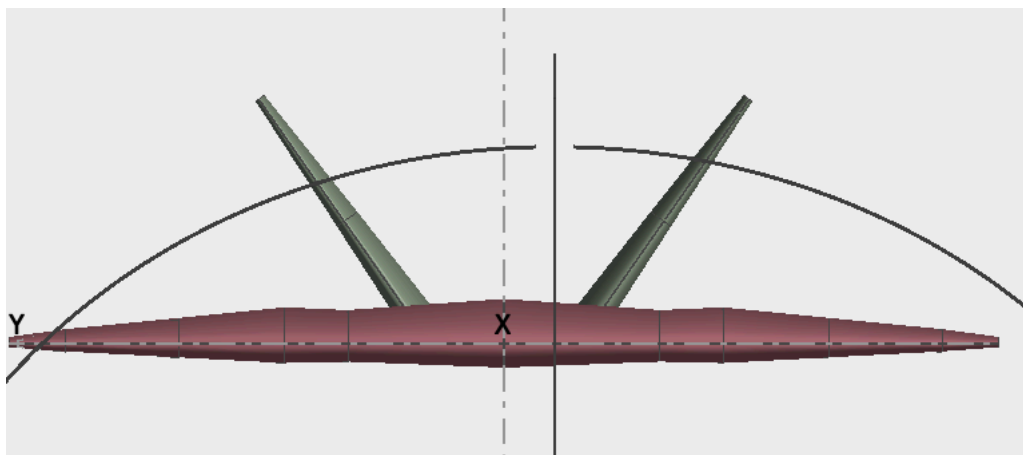
- Now we should define the Analysis of the plane in XFLR5
- Below is the screenshot of the Analysis Setup

Object	Field	Value	Unit
Polar Name	Name	T1-200.0 m/s-VLM2	
⌄ Polar Type			
	Type	FIXEDSPEEDPOLAR	
	Velocity	200.00	m/s
	Alpha	0	°
	Beta	0	°
⌄ Analysis Type			
	Method	VLMMETHOD	
	Boundary condition	DIRICHLET	
	Viscous	true	
	Tilted geometry	false	
	Ignore body panels	true	
⌄ Inertia			
	Use plane inertia	true	
	Mass	19,703.0	kg
⌄ Center of Gravity			
	x	5.947	m
	z	0.256	m
⌄ Inertia tensor			
	Ixx	131,584.5	kg.m²
	Iyy	123,869.3	kg.m²
	Izz	245,174.2	kg.m²
	Ixz	2,398.2	kg.m²
⌄ Reference Dimensions			
	Reference dimensions	PLANFORMREFDIM	
	Reference Area	66.117	m²
	Reference Span Length	13.300	m
	Reference Chord Length	5.567	m
⌄ Environment data			
⌄ Air data			
	Density	1.225	kg/m3
	Viscosity	1.5e-05	m²/s
⌄ Ground height data			
	Ground effect	false	
	Height flight	0	m
⌄ Stability Controls			

Object	Field	Value	Unit
	Reference Area	66.117	m²
	Reference Span Length	13.300	m
	Reference Chord Length	5.567	m
⌄ Environment data			
⌄ Air data			
	Density	1.225	kg/m3
	Viscosity	1.5e-05	m²/s
⌄ Ground height data			
	Ground effect	false	
	Height flight	0	m
⌄ Stability Controls			
⌄ Mass gains			
	Mass	0	kg/ctrl
	CoG.x	0	m/ctrl
	CoG.z	0	m/ctrl
	Ixx	0	kg.m²/ctrl
	Iyy	0	kg.m²/ctrl
	Izz	0	kg.m²/ctrl
	Ixz	0	kg.m²/ctrl
⌄ Angle gains			
	Wing Tilt	0	°/ctrl
	Elevator Tilt	0	°/ctrl
	Wing Flap 1	0	°/ctrl
	Wing Flap 2	0	°/ctrl
	Wing Flap 3	0	°/ctrl
	Wing Flap 4	0	°/ctrl
	Wing Flap 5	0	°/ctrl
	Wing Flap 6	0	°/ctrl
	Wing Flap 7	0	°/ctrl
	Wing Flap 8	0	°/ctrl
	Elevator Flap 1	0	°/ctrl
	Elevator Flap 2	0	°/ctrl
	Elevator Flap 3	0	°/ctrl
	Elevator Flap 4	0	°/ctrl
	Fin Flap 1	0	°/ctrl
	Fin Flap 2	0	°/ctrl
	Fin Flap 3	0	°/ctrl
	Fin Flap 4	0	°/ctrl

- For now, I am leaving stability controls as zero. We can add them later in the project as needed.

- Now I am Analysing for the angle of attack range of -3 degrees to +3 degrees with a step of half a degree.
- The result of the Analysis is Graphically shown in the below Screenshot.

ail 1
```
    =      13.300 m
n  =      13.300 m
   =      66.117 m²
a  =      66.117 m²
   =   19703.000 kg
```
V
Alpha
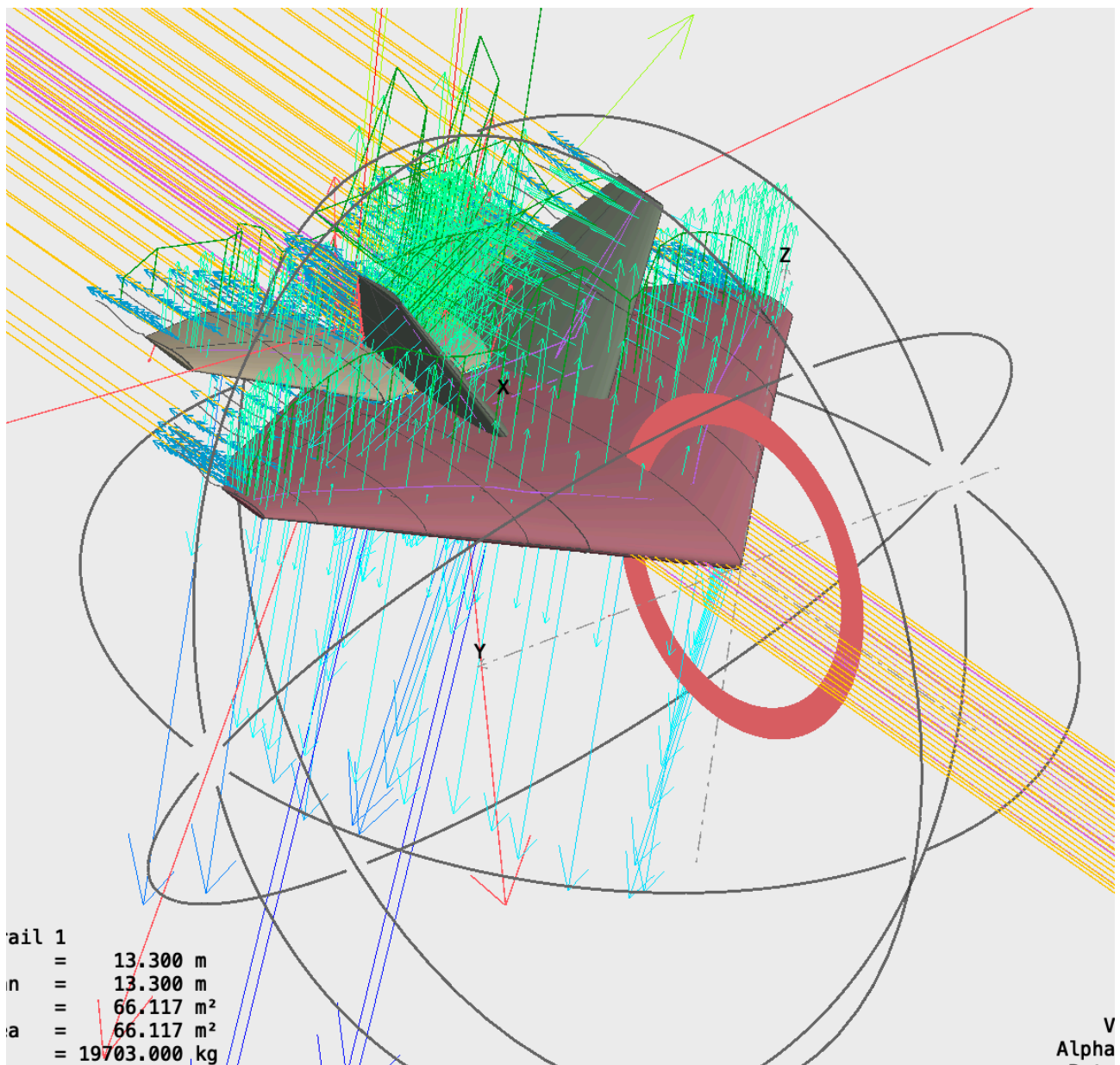
- In this stage of Analysis, we obtain the critical coefficients like C_L, C_D, C_m etc. which are crucial for the next stages of the Analysis.
- Next, we are going to set up stability analysis to obtain Longitudinal and Lateral Stability Derivatives.
- The setup example is shown in the screenshot below. The Analysis is generally defined for the alpha value range but as the controls are zero for now, they would remain the same for any Alpha value.

- Now we obtain Non-Dimensional Stability Derivatives for both Longitudinal And Lateral analysis.
- The XFLR5 gives us the state space model for our plane which can be decoupled to get the A and B matrices.
- The Detailed Description of these Matrices is Given in Appendix C.
- The Matrices are as Follows

Longitudinal Analysis

- For Longitudinal Analysis state space matrices are

$$
A = \begin{bmatrix} -0.13653 & 12.696 & -32.2 & 0 & 0 \\ -0.0042 & -3.0366 & 0 & 1 & 0 \\ 0 & 0 & 0 & 1 & 0 \\ 0.00315 & -13.916 & 0 & -7.68925 & 0 \\ 0 & -352 & 352 & 0 & 0 \end{bmatrix} \qquad B = \begin{bmatrix} 0 & 0.0234 \\ -0.48 & 0 \\ 0 & 0 \\ -16.5435 & 0 \\ 0 & 0 \end{bmatrix}
$$

$$
C = \begin{bmatrix} 1 & 0 & 0 & 0 & 0 \\ 0 & 1 & 0 & 0 & 0 \\ 0 & 0 & 1 & 0 & 0 \\ 0 & 0 & 0 & 1 & 0 \\ 0 & 0 & 0 & 0 & 1 \end{bmatrix} \qquad D = \begin{bmatrix} 0 & 0 \\ 0 & 0 \\ 0 & 0 \\ 0 & 0 \\ 0 & 0 \end{bmatrix}
$$

- Now Using the Matlab Code given by Prof. Terry Hart for Navion Longitudinal Simulation and replacing the model with the state space model above, we obtain the following results.
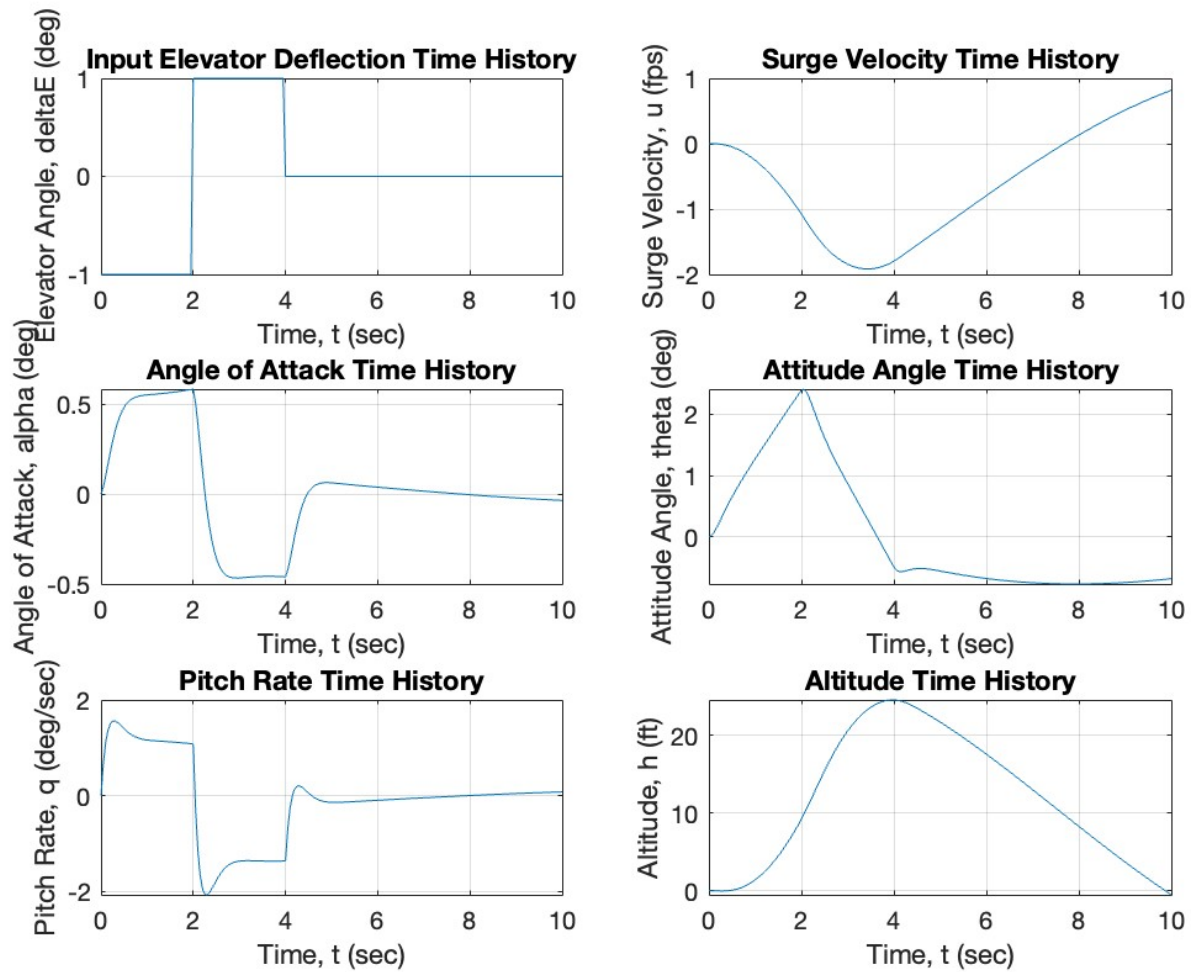
- These results are almost Identical to the results given in the textbook for the Longitudinal simulation.
- It is now, moving on to the Lateral Simulation.

Lateral Analysis

- The State Space Model for the Lateral Simulation is given by

$$
A = \begin{bmatrix}
-0.07568 & 0.275 & 0 & -1 & 0 \\
0 & 0 & 1 & 0 & 0 \\
-23.973 & 0 & -10.0824 & 3.2895 & 0 \\
8.99 & 0 & -0.3498 & -0.6084 & 0 \\
0 & 0 & 0 & 1 & 0
\end{bmatrix}
\qquad
B = \begin{bmatrix}
0 & 0.08465 \\
0 & 0 \\
34.7808 & 3.0576 \\
-0.4436 & -9.194 \\
0 & 0
\end{bmatrix}
$$

$$C = \begin{bmatrix} 1 & 0 & 0 & 0 & 0 \\ 0 & 1 & 0 & 0 & 0 \\ 0 & 0 & 1 & 0 & 0 \\ 0 & 0 & 0 & 1 & 0 \\ 0 & 0 & 0 & 0 & 1 \end{bmatrix} \qquad D = \begin{bmatrix} 0 & 0 \\ 0 & 0 \\ 0 & 0 \\ 0 & 0 \\ 0 & 0 \end{bmatrix}$$

- Inserting this State Space model into the Matlab Code Provided by Prof. Terry Hart yields the following Result
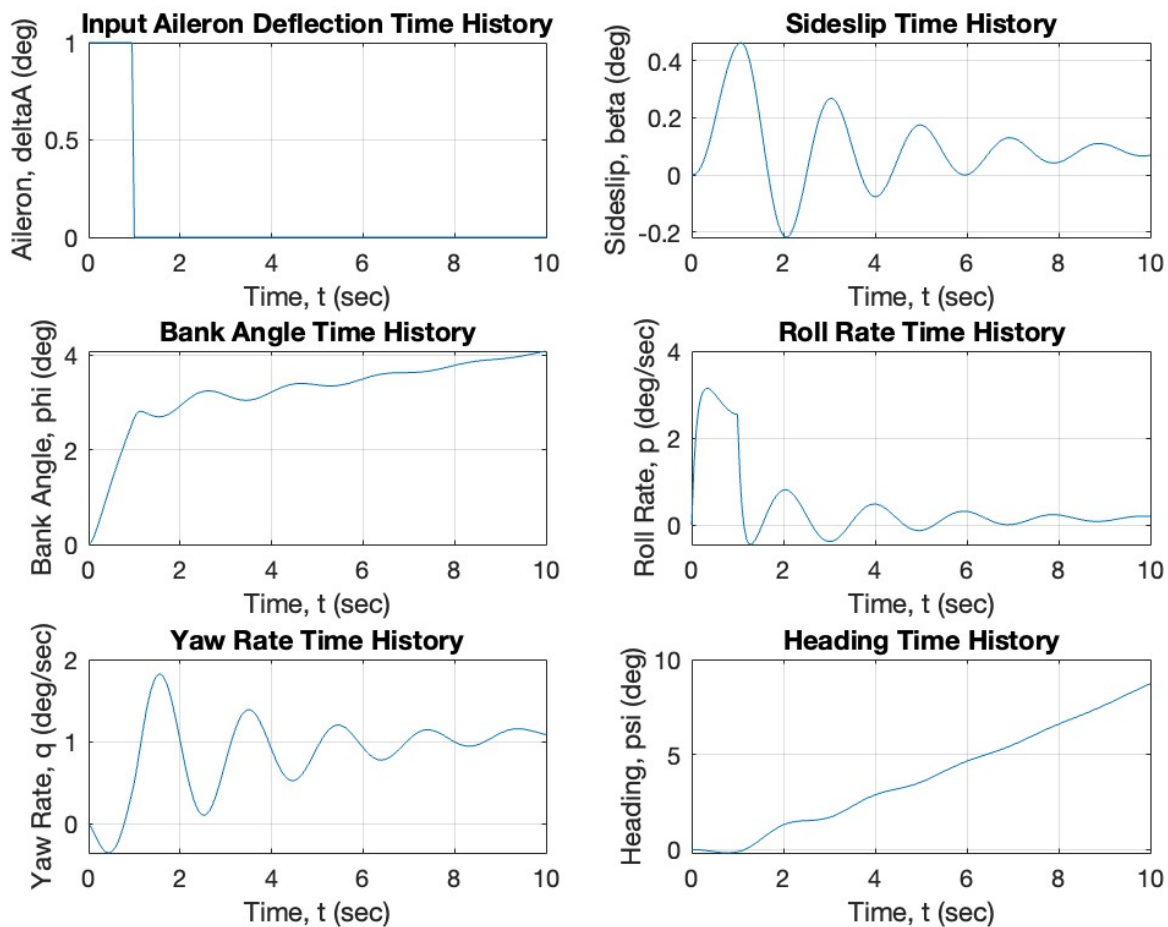
Graphs from Longitudinal Analysis

<u>1. Input Elevator Deflection Time History:</u>
   - Shows a single, sharp negative deflection at the start, suggesting an elevator input that rapidly returns to neutral. This is consistent with a momentary pitch-down command.

<u>2. Surge Velocity Time History:</u>

- Indicates a gradual increase in forward velocity. This could result from the momentary pitch-down, reducing drag and allowing the aircraft to accelerate forward.

3. Angle of Attack Time History:
   - Displays an initial spike followed by oscillations that gradually damp out. The initial response is to the elevator deflection, with subsequent oscillations reflecting the aircraft's return to stable flight.

4. Attitude Angle (Theta) Time History:
   - Shows a sharp increase, a reversal, and a smaller, damped oscillation. It represents the aircraft's nose pitching down and then up in response to the elevator deflection and the natural stability of the aircraft.

5. Pitch Rate Time History:
   - The graph shows an initial negative pitch rate (nose down), followed by a positive pitch rate (nose up), and then oscillations that decrease over time.

6. Altitude Time History:
   - Reflects an overall increase in altitude with an initial dip. The dip corresponds to the pitch-down manoeuvre, while the overall climb may result from the increased speed and subsequent pitch-up.

Graphs from Lateral Analysis

1. Input Aileron Deflection Time History:
   - Shows a brief positive deflection, indicating a momentary roll command to the right. This input is likely to initiate a roll manoeuvre.

2. Sideslip Time History:
   - The sideslip angle varies around zero, suggesting that the aircraft experiences some side-to-side motion relative to its forward path, likely induced by the aileron input.

3. Bank Angle Time History:
   - Increases steadily, reflecting a roll to the right due to the aileron deflection. The bank angle does not return to zero within the displayed time, implying a sustained roll attitude.

4. Roll Rate Time History:
   - Shows an initial spike corresponding to the aileron deflection, followed by a return to near zero. This depicts the initial roll rate induced by the aileron, then a decrease as the bank angle stabilizes.

5. Yaw Rate Time History:
   - Exhibits an oscillatory response with decreasing amplitude. This suggests the aircraft's yaw motion is initiated by the roll manoeuvre and then stabilizing.

6. Heading Time History:
   - Demonstrates a continuous increase in heading angle, implying that the aircraft is turning to the right over time, consistent with the sustained bank angle.

In both sets of graphs, the initial control deflection leads to a transient response, which gradually transitions to a steady state or a damped oscillatory state. The responses suggest that the aircraft has inherent stability, as the oscillations die out over time without additional control inputs. These graphs are useful for analyzing the stability and control characteristics of the F22 and tuning the flight control system for desired performance.

Conclusion of report 1:

Overall, In Report 1 we covered the basic description of the Aircraft, Airfoil Selection, Airfoil analysis, Plane geometry design, obtaining basic aerodynamic coefficients, deriving stability derivatives, creation of state space model and, plotting the responses for a 2-second elevator doublet and a 1-second aileron input.

In the next phases of the project, we will further improve the Performance of the aircraft by using control theory.

Report - 2

The primary objective of this section of the report is to detail the design and simulation process for pitch and yaw dampers specifically aimed at enhancing the damping of the short-period pitch mode and the Dutch roll mode in an aircraft. This will involve the intricate adjustment of control algorithms to optimize the aircraft's response to disturbances in these critical modes. Initially, the report will outline the theoretical foundations underpinning the control strategies for both dampers. This includes a discussion on the dynamic characteristics of the short-period pitch and Dutch roll modes, highlighting the need for enhanced damping. Subsequently, the report will present the methodology employed in designing the control system, including the selection of control parameters and the rationale behind these choices.

In terms of deliverables, this section will provide comprehensive simulation results that demonstrate the efficacy of the designed pitch and yaw dampers in improving the aircraft's stability and response characteristics. The simulations will showcase how the dampers mitigate adverse dynamics in the targeted modes, backed by comparative data illustrating the performance improvements. Additionally, the report will delve into the analysis of a specific bending mode along the longitudinal axis, including the identification and analysis of aeroelastic stability derivatives associated with this mode. This analysis will further reinforce the importance of the dampers in maintaining the overall structural integrity and dynamic stability of the aircraft, providing a holistic view of the system's enhanced performance capabilities.

Part 1: Pitch Damper and Yaw Damper Design

- In this part, we are designing the pitch and yaw dampers that will make a significant improvement in dampening the short-period pitch mode and the Dutch roll mode for our aeroplane.
- The Matlab script is given in Appendix D, which is described below.

This MATLAB script is designed to analyze and simulate the dynamic responses of an aircraft under both longitudinal and lateral control settings using state-space models. The script provides a comprehensive study of the system's behavior through simulation of control inputs and visualization of the system's response dynamics. Here's a breakdown of the script's functionality:

Longitudinal System Setup

- <u>State-Space Model Definition</u>: The script defines the matrices A, B, C, and D for the longitudinal dynamics of the aircraft, which represent the state dynamics, control input, output matrix, and direct transmission matrix respectively.
- <u>System Augmentation</u>: A feedback loop with a gain K_q is added to the system to simulate the effect of a longitudinal control input, specifically an altitude control doublet. This augmented system uses a transfer function to model an actuator dynamics.
- <u>Control System Analysis</u>: The script evaluates the controllability of the system and visualizes the control effects through root locus and impulse response plots, which help in understanding the stability and responsiveness of the system to control inputs.

Lateral System Setup

- <u>State-Space Model Definition</u>: Similar to the longitudinal system, the lateral dynamics are modelled using corresponding state-space matrices.
- <u>System Augmentation</u>: A feedback gain K_r is applied to modify the system dynamics based on lateral control input, enhancing the roll rate control.
- <u>Control System Analysis</u>: The script checks the controllability and generates root locus and impulse response plots for the lateral system, providing insights into its behavior under modified control conditions.

Simulation of System Response

- <u>Simulation Configuration</u>: Time vector t and initial state x_0 are defined to simulate the system's response over a specified time frame.
- <u>Input Definition</u>: For the lateral system, an aileron deflection input is defined over a one-second interval to observe the aircraft's reaction to lateral maneuvers.
- <u>Response Visualization</u>: The script uses the `lsim` function to simulate the time response of the lateral system to the aileron input. Subsequent plots display various aspects of the aircraft's response, including sideslip, bank angle, roll rate, yaw rate, and heading. These plots are crucial for validating the effectiveness of control strategies and understanding the aircraft's behavior under operational conditions.

Visualization and Debugging

- <u>Plotting</u>: Each section of the script is accompanied by figures that illustrate the system's theoretical and simulated responses. This includes plots for input deflections and their corresponding effects on the aircraft's dynamics.

-<u>Organization</u>: Figures are organized and labeled systematically to facilitate clear and easy interpretation of results.

This script is essential for aerospace engineers and control system analysts, providing a robust framework for simulating and tweaking aircraft dynamics efficiently, thereby aiding in the design of effective control strategies for improving aircraft performance and safety.

The results are as follows

Root Locus

Impulse Response

1 second aileron input (with Gain Input)

Input Aileron Deflection Time History

Sideslip Time History

Bank Angle Time History

Roll Rate Time History

Yaw Rate Time History

Heading Time History
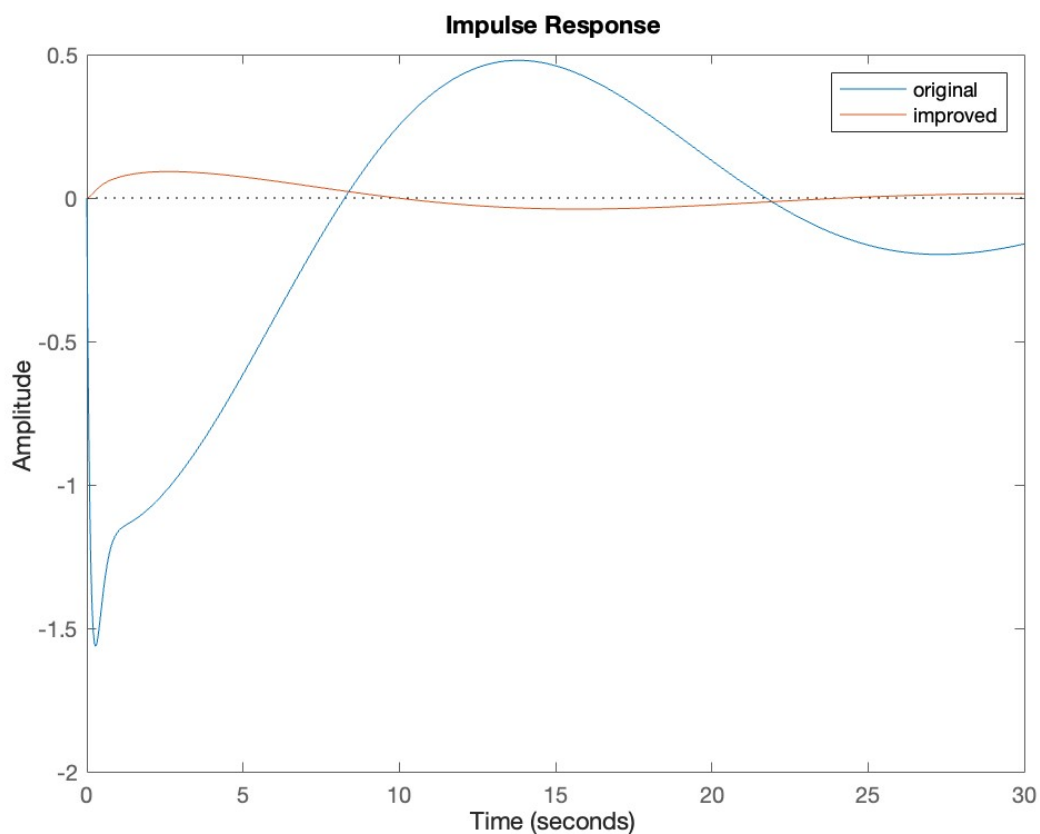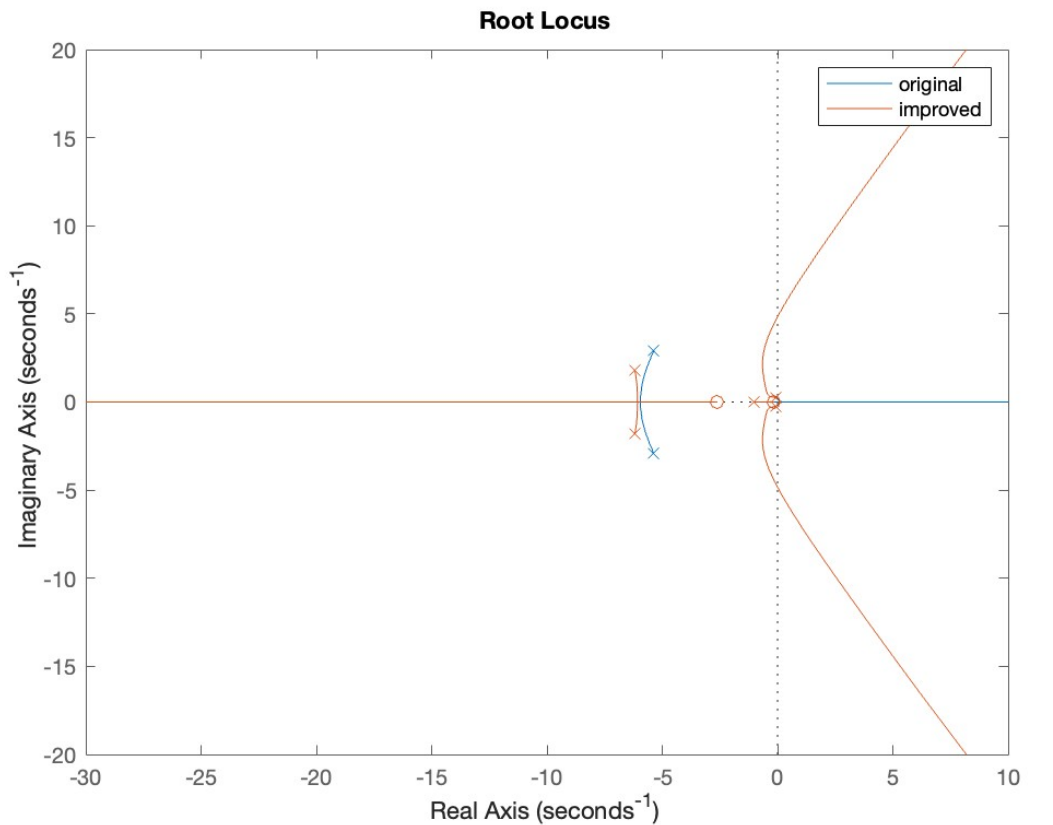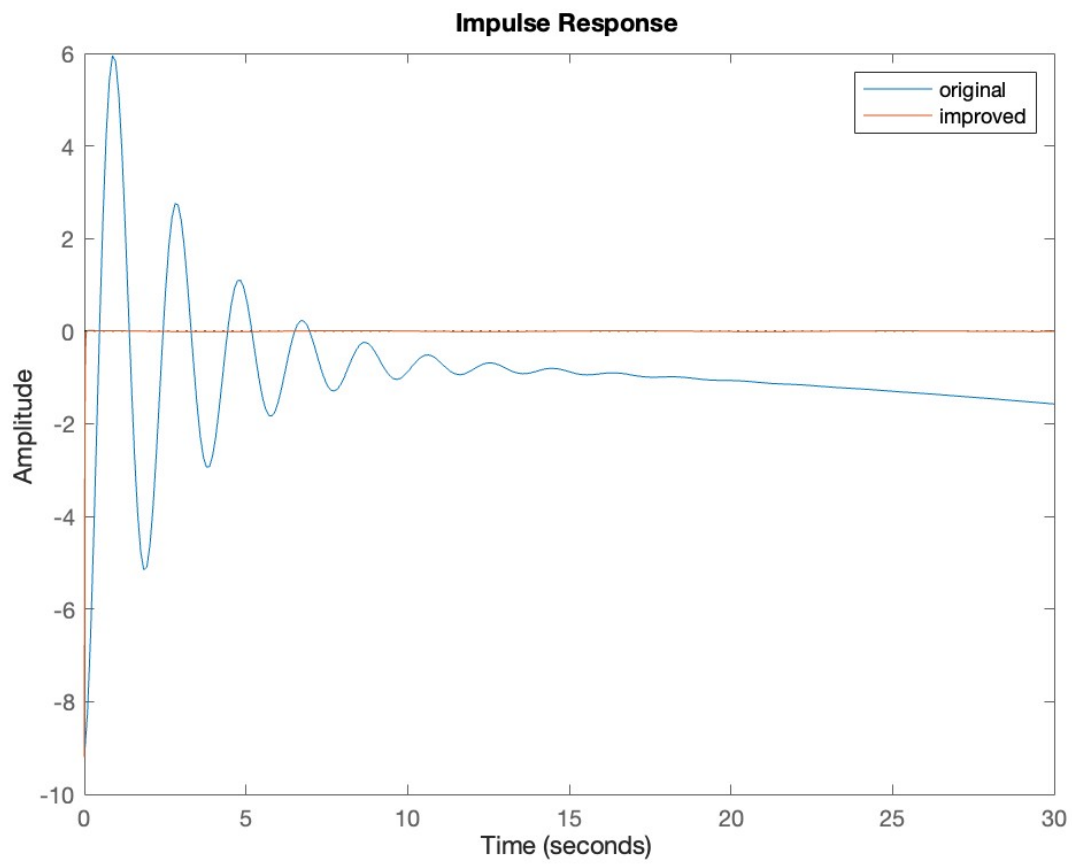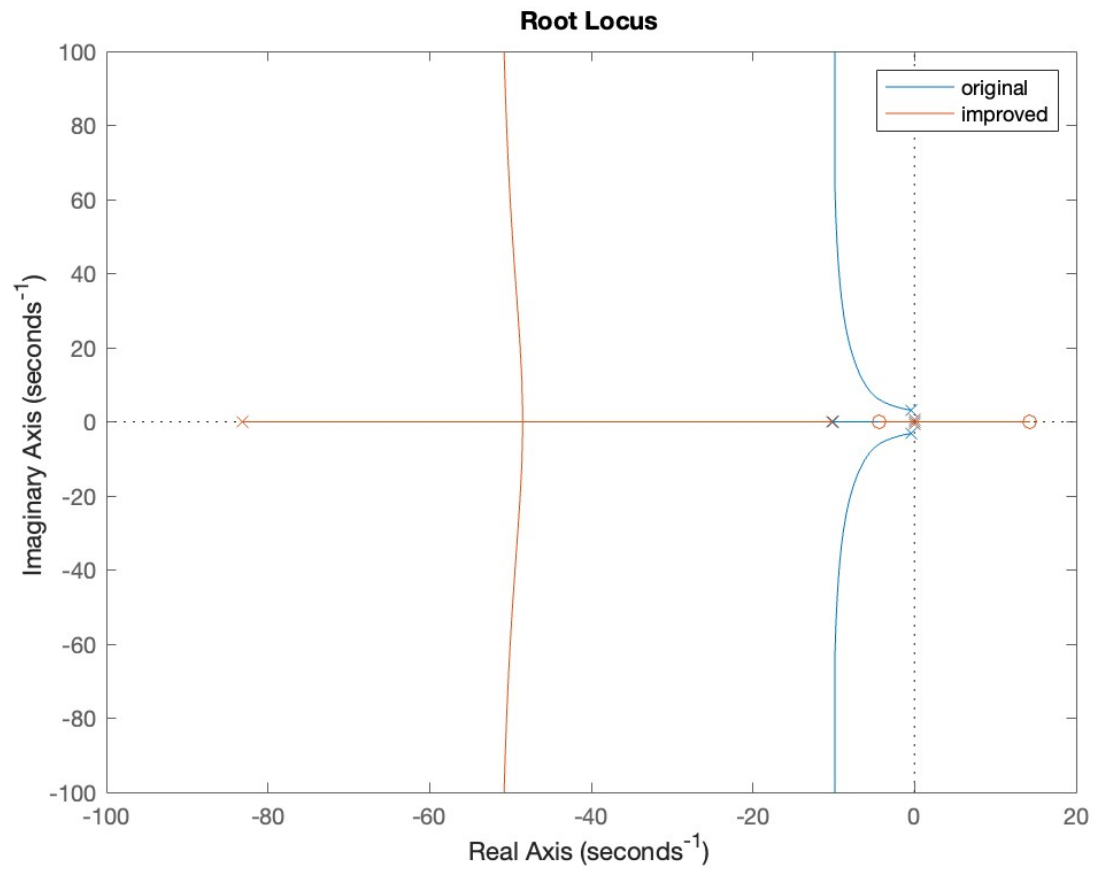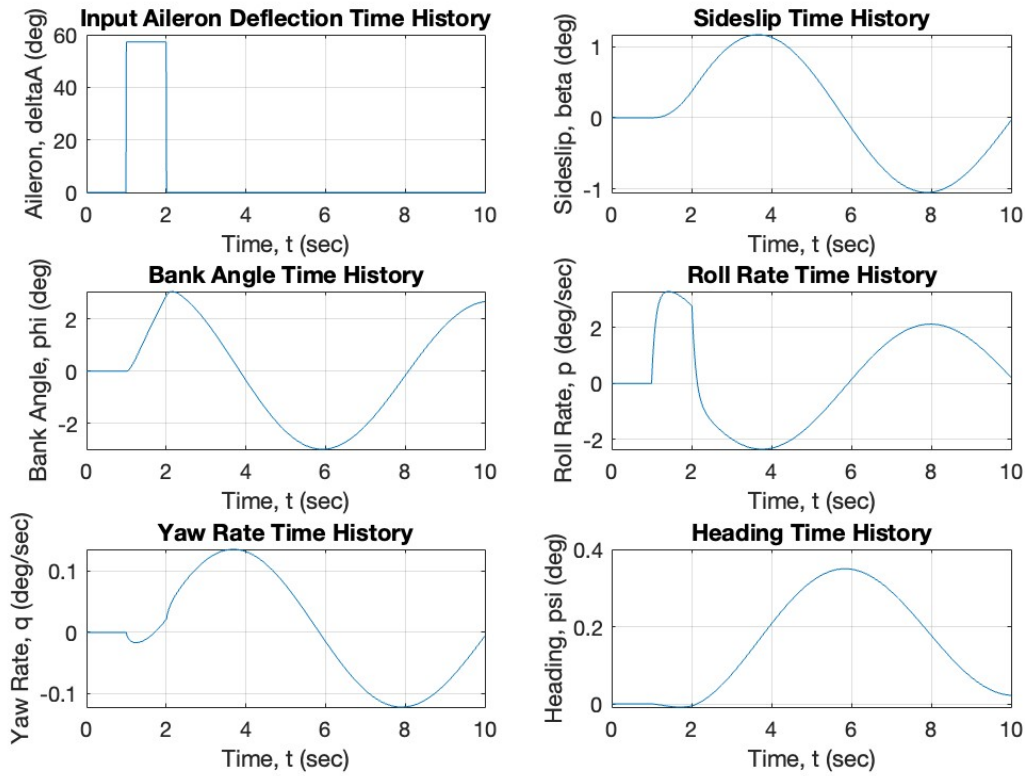
2 second elevator doublet (With Gain Input)

Input Elevator Deflection Time History

Surge Velocity Time History

Angle of Attack Time History

Attitude Angle Time History

Pitch Rate Time History

Altitude Time History
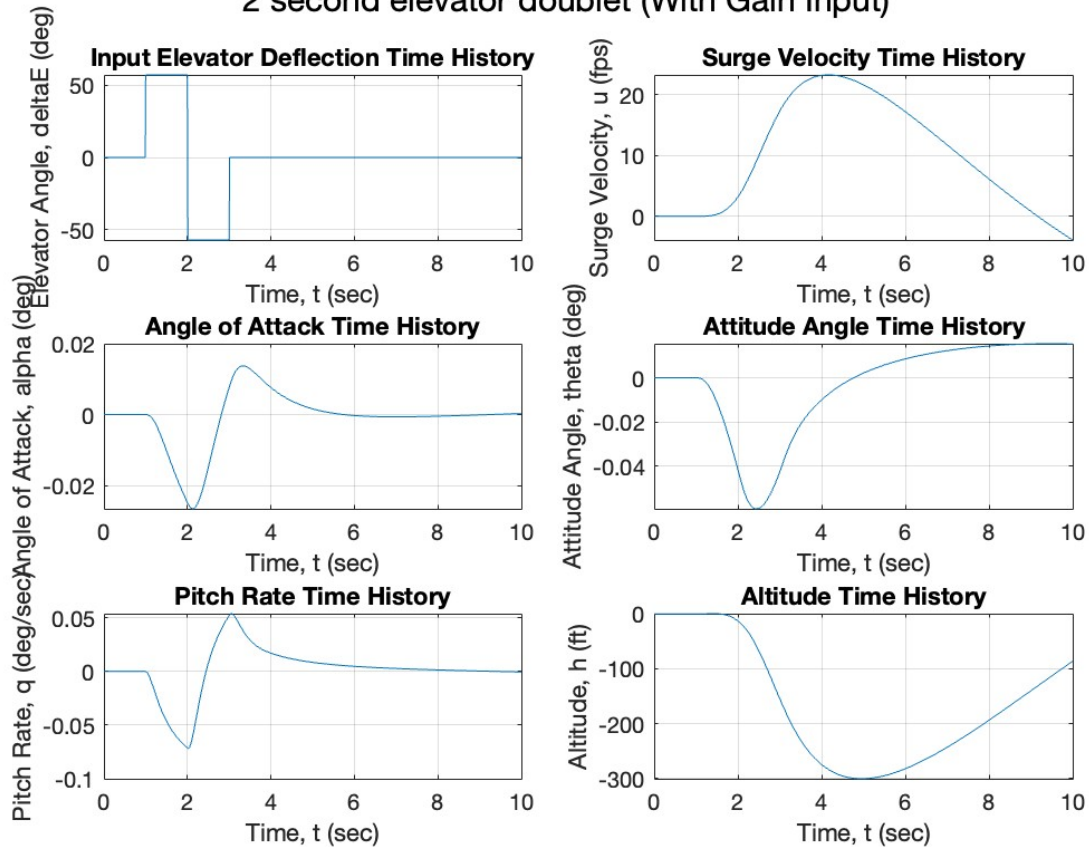
The Transfer Functions are given by,

```
TFLong =

  From input 1 to output...
              -6.094 s^2 + 275.8 s + 1403
  1:  ---------------------------------------
      s^4 + 10.86 s^3 + 38.78 s^2 + 5.559 s + 2.19

          -0.48 s^3 - 20.3 s^2 - 2.763 s - 2.286
  2:  ---------------------------------------
      s^4 + 10.86 s^3 + 38.78 s^2 + 5.559 s + 2.19

              -16.54 s^2 - 45.81 s - 6.848
  3:  ---------------------------------------
      s^4 + 10.86 s^3 + 38.78 s^2 + 5.559 s + 2.19

      -16.54 s^3 - 45.81 s^2 - 6.848 s - 4.293e-16
  4:  ---------------------------------------
      s^4 + 10.86 s^3 + 38.78 s^2 + 5.559 s + 2.19

          169 s^3 + 1322 s^2 - 1.515e04 s - 1606
  5:  ------------------------------------------------
      s^5 + 10.86 s^4 + 38.78 s^3 + 5.559 s^2 + 2.19 s


  From input 2 to output...
          0.0234 s^3 + 0.251 s^2 + 0.872 s
  1:  ---------------------------------------
      s^4 + 10.86 s^3 + 38.78 s^2 + 5.559 s + 2.19

              -9.828e-05 s^2 - 0.000682 s
  2:  ---------------------------------------
      s^4 + 10.86 s^3 + 38.78 s^2 + 5.559 s + 2.19

              7.371e-05 s + 0.001591
  3:  ---------------------------------------
      s^4 + 10.86 s^3 + 38.78 s^2 + 5.559 s + 2.19

              7.371e-05 s^2 + 0.001591 s
  4:  ---------------------------------------
      s^4 + 10.86 s^3 + 38.78 s^2 + 5.559 s + 2.19

          0.03459 s^2 + 0.266 s + 0.5602
  5:  ------------------------------------------------
      s^5 + 10.86 s^4 + 38.78 s^3 + 5.559 s^2 + 2.19 s
```

TFAugLong =

  From input 1 to output...
                     0.6094 s^2 - 27.58 s - 140.3
    1: ---
        s^5 + 13.52 s^4 + 55.88 s^3 + 49.61 s^2 + 8.434 s + 2.19

                   0.048 s^3 + 2.03 s^2 + 0.2763 s + 0.2286
    2: ---
        s^5 + 13.52 s^4 + 55.88 s^3 + 49.61 s^2 + 8.434 s + 2.19

                        1.654 s^2 + 4.581 s + 0.6848
    3: ---
        s^5 + 13.52 s^4 + 55.88 s^3 + 49.61 s^2 + 8.434 s + 2.19

                   1.654 s^3 + 4.581 s^2 + 0.6848 s - 1.008e-16
    4: ---
        s^5 + 13.52 s^4 + 55.88 s^3 + 49.61 s^2 + 8.434 s + 2.19

                   -16.9 s^3 - 132.2 s^2 + 1515 s + 160.6
    5: ---
        s^6 + 13.52 s^5 + 55.88 s^4 + 49.61 s^3 + 8.434 s^2 + 2.19 s

  From input 2 to output...
                    -0.00234 s^3 - 0.02897 s^2 - 0.09739 s
    1: ---
        s^5 + 13.52 s^4 + 55.88 s^3 + 49.61 s^2 + 8.434 s + 2.19

                        9.828e-06 s^2 + 8.481e-05 s
    2: ---
        s^5 + 13.52 s^4 + 55.88 s^3 + 49.61 s^2 + 8.434 s + 2.19

                         -7.371e-06 s - 0.0001591
    3: ---
        s^5 + 13.52 s^4 + 55.88 s^3 + 49.61 s^2 + 8.434 s + 2.19

                        -7.371e-06 s^2 - 0.0001591 s
    4: ---
        s^5 + 13.52 s^4 + 55.88 s^3 + 49.61 s^2 + 8.434 s + 2.19

                     -0.003459 s^2 - 0.03245 s - 0.05602
    5: ---
        s^6 + 13.52 s^5 + 55.88 s^4 + 49.61 s^3 + 8.434 s^2 + 2.19 s

Here are descriptions for each of the images based on the context and typical contents of such figures in control system analysis:

Impulse Response
This image shows the impulse response of an aircraft control system, comparing the original system with an improved version. The graph plots amplitude against time (in seconds) and clearly illustrates the differences in the transient responses:
- Original System: Exhibits significant oscillations before gradually settling.
- Improved System: Shows a damped response, quickly stabilizing to a steady state, indicating better control effectiveness and system stability.

Root Locus
This root locus plot illustrates the path of the closed-loop poles of the control system as a function of gain values. It compares the original and improved system designs:
- Original System: The poles start further to the right in the s-plane, suggesting slower response characteristics.
- Improved System: The poles quickly move towards the left half of the s-plane as the gain increases, indicating a faster and more stable system response.

Impulse Response for Different Output
This graph represents another impulse response for a different output or configuration of the same control system, showing the original and improved system responses:
- Original System: Gradually approaches a zero value from below, indicating a possible overshoot and slower settling time.
- Improved System: Shows a smoother and quicker approach to zero, demonstrating a more controlled and stable response.

Root Locus for Different Control Configuration
This root locus plot demonstrates the system's stability under a different control configuration or for a different system output:
- Original System: Shows poles that are closer to the imaginary axis, indicating marginal stability.
- Improved System: Shows that the poles move further left into the s-plane with increasing gain, indicating enhanced stability.

Elevator Doublet Response
This set of plots displays various dynamic responses of the aircraft to a "2-second elevator doublet" control input:
- Input Elevator Deflection: Shows a sharp change in control input and its reversal.
- Surge Velocity: Exhibits a symmetric increase and decrease around the input.
- Angle of Attack, Attitude Angle, Pitch Rate, and Altitude: All these plots show the temporal evolution of the aircraft's responses to the input, emphasizing the transient dynamics and the effects of the control input over time.

Aileron Input Response
This collection of graphs details the response of the aircraft to a "1-second aileron input":
- Input Aileron Deflection: Marks the brief period of aileron deflection.
- Bank Angle, Sideslip, Roll Rate, Yaw Rate, and Heading: These graphs highlight how the aircraft's lateral motion and orientation are affected by the control input, showing key performance metrics in response to the maneuver.

Part 2 :

Defining a bending mode in the longitudinal axis of an aircraft and determining the aeroelastic stability derivatives for that mode involves several critical steps that integrate the disciplines of structural dynamics and aerodynamics. XFLR5 takes care of most of the process. Here's a detailed breakdown of the process.

1. <u>Modal Analysis of the Structure</u>: The first step involves performing a modal analysis on the aircraft structure to identify its natural frequencies and mode shapes. In this case, the focus is on the bending modes in the longitudinal axis. This analysis typically uses finite element methods (FEM) to model the structure and calculate its dynamic characteristics. The output includes various mode shapes, of which the bending modes relevant to longitudinal motion are selected.

2. <u>Aerodynamic Loading Analysis</u>: Once the bending mode is identified, the next step is to analyze how aerodynamic forces affect this mode. This involves computing the unsteady aerodynamic forces and moments acting on the structure when it deforms according to the selected bending mode shape. Methods such as Theodorsen's theory for thin airfoils or more complex computational fluid dynamics (CFD) simulations may be employed depending on the accuracy required and the complexity of the aircraft geometry.
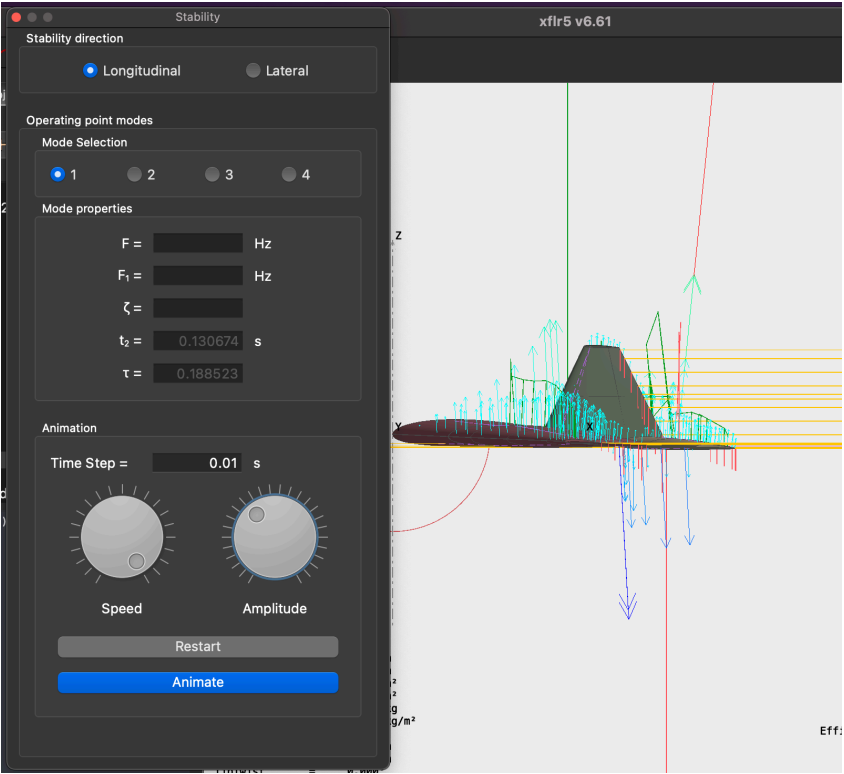
3. <u>Coupling Structure and Aerodynamics</u>: With the structural and aerodynamic data, the next step involves coupling these two aspects to form an aeroelastic model. This is typically done using state-space or transfer function approaches, where the aerodynamic forces are expressed as functions of the structural displacements and velocities.

4. <u>Determination of Aeroelastic Stability Derivatives</u>: Aeroelastic stability derivatives are then calculated from the coupled aeroelastic model. These derivatives, which include terms like the flutter derivative, pitch damping derivative, and others, quantify how changes in aerodynamic forces and moments are affected by changes in the bending mode's motion. Stability derivatives are crucial for predicting the aeroelastic stability of the aircraft.

5. <u>Stability Analysis</u>: Finally, using the obtained aeroelastic stability derivatives, perform a stability analysis to assess the dynamic stability of the aircraft. This involves evaluating the roots of the characteristic equation of the aeroelastic system to determine whether they lie in the left half of the complex plane, indicating stable behavior. Unstable modes need further redesign or control strategies to mitigate.

This integrated approach ensures a comprehensive understanding of how structural deformations in flight affect aircraft stability and performance, leading to safer and more efficient aircraft designs.

The XFLR5 can do Flex body analysis for both Longitudinal and Lateral Modes, following is the screenshot of the Animation of Mode 1 of the longitudinal Analysis.

- Similar to the rigid body state space model we can obtain an aeroelastic stability model for the F22 Raptor, which can then be Decoupled to obtain the A and B matrices for this model.

$$
A_{\text{flex}} = \begin{bmatrix}
-0.13653 & 12.696 & -32.2 & 0 & 0 & 0 & 0 \\
-0.0042 & -3.0366 & 0 & 1 & 0 & -0.00634 & -0.000340 \\
0 & 0 & 0 & 1 & 0 & 0 & 0 \\
0.00315 & -13.916 & 0 & -7.68925 & 0 & -0.1003 & -0.560 \\
0 & -352 & 352 & 0 & 0 & 0 & 0 \\
0 & 0 & 0 & 0 & 0 & 0 & 1 \\
0 & 0 & 0 & 0 & 0 & -225.3 & -1.342
\end{bmatrix}
$$

$$
B_{\text{flex}} = \begin{bmatrix}
0 & 0.0234 \\
-0.48 & 0 \\
0 & 0 \\
-16.5435 & 0 \\
0 & 0 \\
0 & 0 \\
-564 & 0
\end{bmatrix}
$$

$$
C_{\text{flex}} = \begin{bmatrix}
1 & 0 & 0 & 0 & 0 & 0 & 0 \\
0 & 1 & 0 & 0 & 0 & 0 & 0 \\
0 & 0 & 1 & 0 & 0 & 0 & 0 \\
0 & 0 & 0 & 1 & 0 & 0 & 0 \\
0 & 0 & 0 & 0 & 1 & 0 & 0 \\
0 & 0 & 0 & 0 & 0 & 1 & 0 \\
0 & 0 & 0 & 0 & 0 & 0 & 1
\end{bmatrix}
$$

$$
D_{\text{flex}} = \begin{bmatrix}
0 & 0 \\
0 & 0 \\
0 & 0 \\
0 & 0 \\
0 & 0 \\
0 & 0 \\
0 & 0
\end{bmatrix}
$$

- Now we can compare the results of the rigid body assumption to that of the Flex body. The Matlab Code is given in the Appendix. The Explanation of the code is as follows

The MATLAB code simulates the response of an aircraft in two configurations: a "rigid body" and a "flex body", under the same elevator deflection inputs. Here's a summary of the different parts and what they do:

1. Definition of System Matrices:
   - Rigid Body Configuration:
      - `A_rigid`, `B_rigid`, `C_rigid`, and `D_rigid` matrices define the state-space model of the rigid body aircraft dynamics.
     - `sys_rigid` constructs the state-space object for this configuration.
     - Flex Body Configuration:
     - `A_flex`, `B_flex`, `C_flex`, and `D_flex` matrices, which include additional states for the flexible modes of the aircraft.
     - `sys_flex` constructs the state-space object for the flexible configuration.

2. Simulation Setup:
     - `t` defines the simulation time vector from 0 to 10 seconds in increments of 0.05 seconds.
     - `u` sets up the input matrix for the elevator angle, which is manipulated in two phases: first a negative deflection for 2 seconds, then a positive deflection for another 2 seconds, both small magnitude, simulating pilot input or automatic control adjustments.

3. Simulation Execution:
     - `y_rigid` and `y_flex` are the outputs from the simulations for the rigid and flex body configurations, respectively, using the `lsim` function which simulates the time response of linear systems.

4. Plotting Results:
     - The code plots various response characteristics of both configurations, laid out in two figures.
     - For the rigid body:
     - Elevator angle, surge velocity, angle of attack, attitude angle, pitch rate, and altitude.
     - For the flex body:
     - The same outputs as the rigid body, plus additional plots for the first mode displacement and velocity, reflecting the aircraft's flexible body dynamics.

This MATLAB script essentially compares how the flex body's additional degrees of freedom affect typical response parameters under the same control inputs, giving insight into the dynamic characteristics of an aircraft incorporating the effects of structural flexibility.

- The Results of the code are as follows,
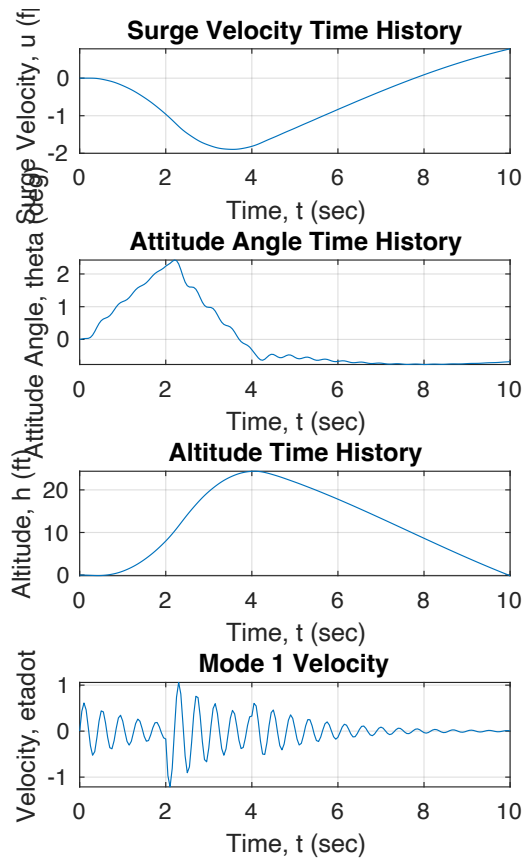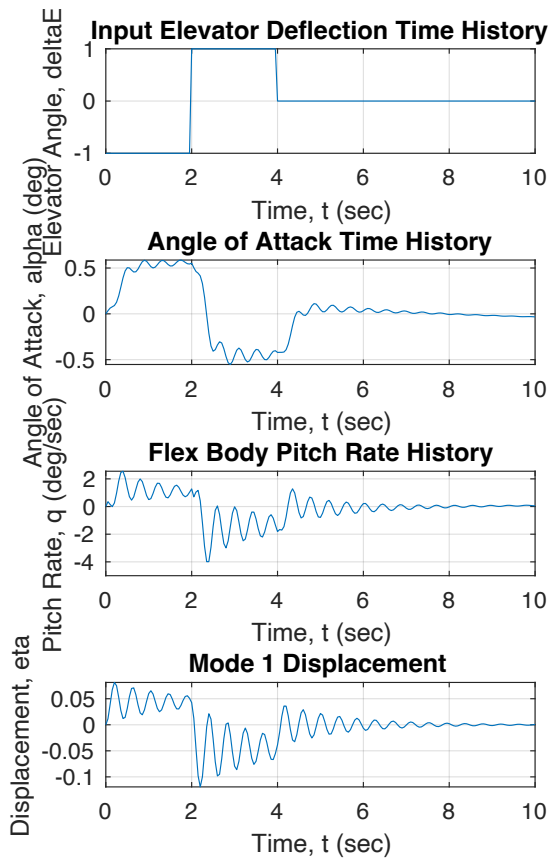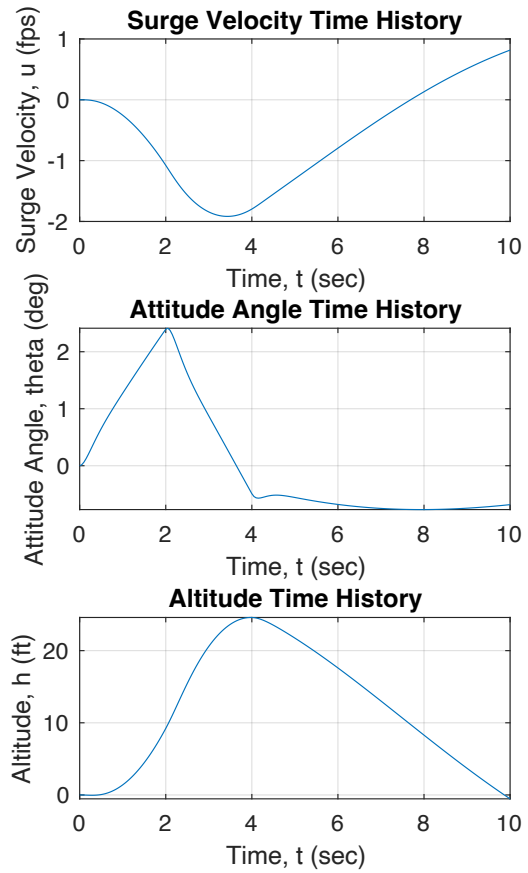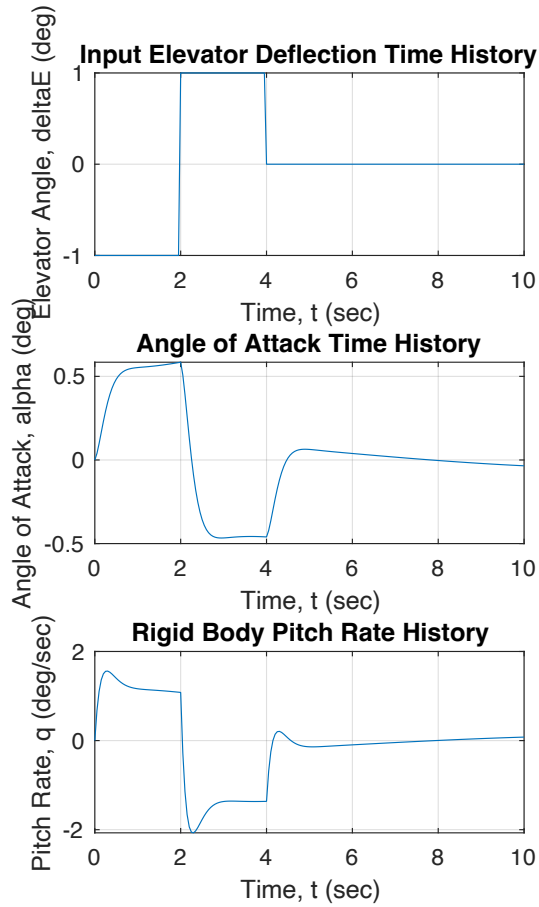
The graphs provided showcase the dynamic response of an aircraft's rigid body and flex body models to certain inputs and system characteristics over a time span of 10 seconds. Let's analyze and compare the two sets of graphs to understand the differences in behavior between the rigid and flex body models.

Graphs for Rigid Body Model

1. <u>Input Elevator Deflection Time History</u>: This graph shows a step input that changes at about 2 seconds and returns to zero at around 4 seconds. The input is the elevator deflection which controls the pitch of the aircraft.
2. <u>Surge Velocity Time History</u>: The surge velocity gradually increases, suggesting a constant acceleration as a result of the elevator input affecting the aircraft's pitch and subsequently its velocity.
3. <u>Angle of Attack Time History</u>: There's an initial sharp increase and decrease in the angle of attack corresponding to the changes in elevator deflection, stabilizing shortly after.
4. <u>Attitude Angle Time History</u>: The attitude angle shows a noticeable peak which correlates with the input deflection. This peak indicates a change in the nose attitude of the aircraft, returning to a lower stable state after the input ceases.
5. <u>Pitch Rate History</u>: Displays sharp peaks that coincide with changes in elevator deflection, indicating rapid changes in pitch rate during these periods.
6. <u>Altitude Time History</u>: Shows a progressive increase in altitude, which makes sense given the positive surge velocity and the attitude changes affecting the aircraft's lift.

Graphs for Flex Body Model

1. <u>Input Elevator Deflection Time History</u>: Identical to the rigid body model, showing the same step changes in elevator input.
2. <u>Surge Velocity Time History</u>: Similar trend as the rigid body, but smoother, suggesting that the flex body dynamics dampen the velocity response slightly.
3. <u>Angle of Attack Time History</u>: Displays more fluctuation compared to the rigid body model, indicating that the flexing of the body affects the angle of attack more dynamically.
4. Attitude Angle Time History: Less pronounced peaks compared to the rigid body, showing that the flex body absorbs some of the changes in attitude.
5. <u>Pitch Rate History</u>: In contrast to the rigid body, the flex body shows ongoing oscillations in pitch rate, indicative of the flexing modes interacting with the aerodynamic controls.
6. <u>Altitude Time History</u>: The trend in altitude gain is similar to the rigid body but appears smoother.
7. <u>Mode 1 Displacement and Mode 1 Velocity</u>: These new graphs show the displacement and velocity of the first mode of the structure's bending. The displacement shows oscillations that decay over time, while the velocity graph shows these oscillations with varying amplitude, both of which indicate the dynamic response of the aircraft structure to aerodynamic loads and control inputs.

Comparison

- The rigid body model reacts more sharply to control inputs, as seen in the pitch rate and angle of attack graphs.
- The flex body model demonstrates additional dynamic behaviors such as oscillations in the pitch rate and mode-specific responses (displacement and velocity of Mode 1), which are not present in the rigid body model.

- Both models exhibit similar trends in surge velocity and altitude, but the flex body responses are generally smoother and show more complex dynamics due to the structural flexibility.

In conclusion, the flex body model introduces additional complexity and realism into the simulation, capturing the effects of structural dynamics on the aircraft's overall behavior, which are crucial for accurate modelling of real-world aircraft performance.
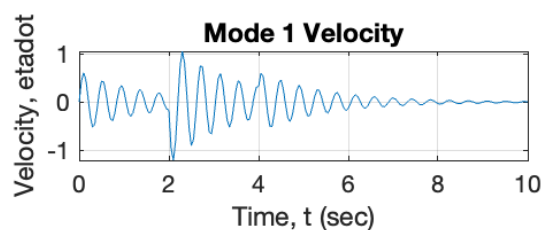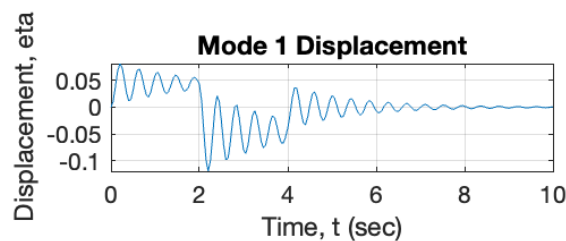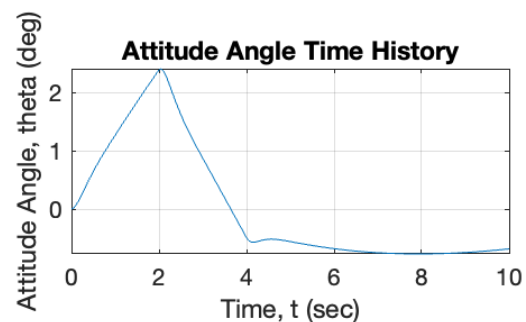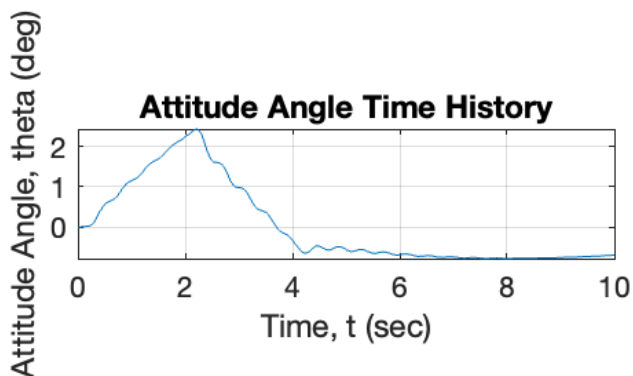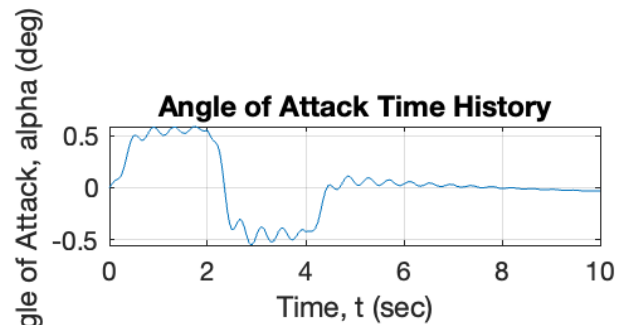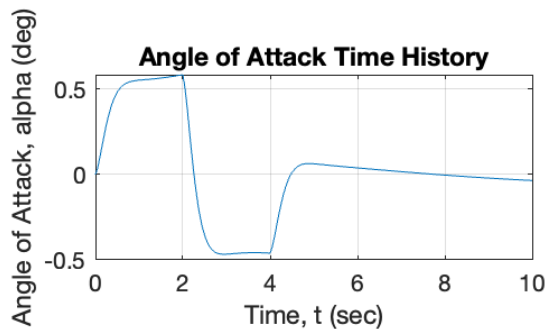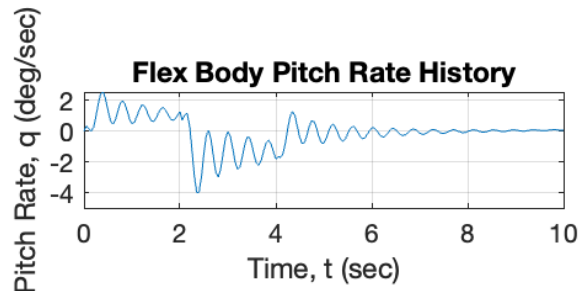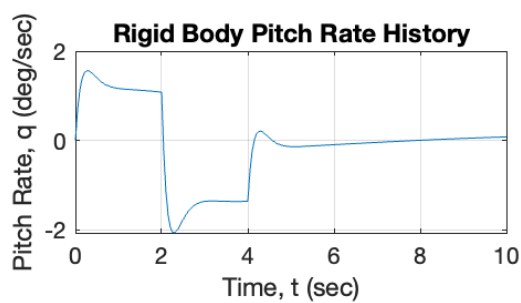
Report 2 Conclusion:

Overall, in Report 2 Using the models we developed for the first report, we successfully designed pitch and yaw dampers that made a significant improvement in dampening the short-period pitch mode and the Dutch roll mode for our aeroplane and we defined bending mode 1 in the longitudinal axis, and determined the aeroelastic stability derivatives for that mode. We also compared the results of aeroelastic analysis to those of rigid body analysis. In the next part we will improve our aircraft further by using the data we have analysed so far.

Report - 3

In this report, we explore the design and analysis of advanced control systems for F-22 Raptor fighter jet model, focusing on the implementation of autopilots for altitude and heading hold, alongside a damping mechanism for longitudinal bending mode vibrations. The primary objective of the altitude hold autopilot is to maintain a constant altitude in response to external disturbances or commanded changes, thereby stabilizing the aircraft's vertical flight path. Concurrently, the heading hold autopilot is aimed at maintaining or adjusting the aircraft's heading to a specified directional angle, crucial for navigational accuracy and mission alignment. The integration of these autopilots not only enhances the operational efficiency and safety of the aircraft but also ensures robust performance in dynamic environments.

Furthermore, addressing the aeroelastic phenomena characteristic of high-performance aircraft, we propose the design of a damper using the elevator control surface to mitigate vibrations inherent in the longitudinal bending mode. This damping strategy is vital for maintaining structural integrity and preventing potential resonant failures due to aerodynamic forces. Through detailed modeling and simulation, we evaluate the response of the aircraft to step changes—a 100-foot increase in altitude and a 3-degree change in heading. These simulations help in fine-tuning the control systems to achieve desired performance metrics, ensuring that the aircraft adheres to the stringent stability and control requirements typical in advanced fighter jets. The effectiveness of the longitudinal damper is demonstrated through its impact on the aircraft's dynamic response, highlighting the critical role of control system design in enhancing aeroelastic stability.

part1

The Matlab code for autopilot design is given in the appendix

The Description of the code is as follows

The MATLAB code outlines the process of designing an autopilot for altitude hold in an aircraft control system. The script begins by defining a constant, `U0`, which represents a baseline speed or a specific operational parameter necessary for the control system calculations. This value needs to be substituted with an actual value relevant to the specific aircraft being modeled.

The code then proceeds to extract the zero-pole-gain (ZPK) data from the augmented system's outputs. It uses MATLAB's `zpkdata` function to obtain zeros, poles, and gain values from specific transfer functions of the augmented longitudinal dynamics system, `sysAugLong`. The data extracted from the second and third outputs to the first input of `sysAugLong` are used to design the altitude hold controller.

The controller design utilizes these zero-pole-gain data to configure a compensator `gammatheta`, which is essentially a transfer function representing the control strategy to maintain altitude. This compensator is further combined with other transfer function elements, including `hgamma`, a scaling transfer function proportional to `U0`, and `pi` and `lc`, two compensatory transfer functions designed to tune the controller's response to desired dynamics.

The product of these transfer functions (`Kh * pi * lc * gammatheta`), scaled by `Kh` (a tuning parameter), forms the core control system, which is then cascaded with `hgamma` to create the complete altitude control system `sys`. This system is converted to a state-space model, which is then adjusted to form a closed-loop system `sysclalt` by modifying its A matrix through state feedback.

Finally, the code executes a simulation to display the step response of the system to a 100-foot altitude change using MATLAB's `step` function with a specified step amplitude. It also provides a Bode plot of the system to analyze its frequency response characteristics. Both plots are crucial for evaluating the performance and stability of the altitude hold autopilot under the designed control laws.

Altitude Hold Bode Plot

Altitude Hold Step Response
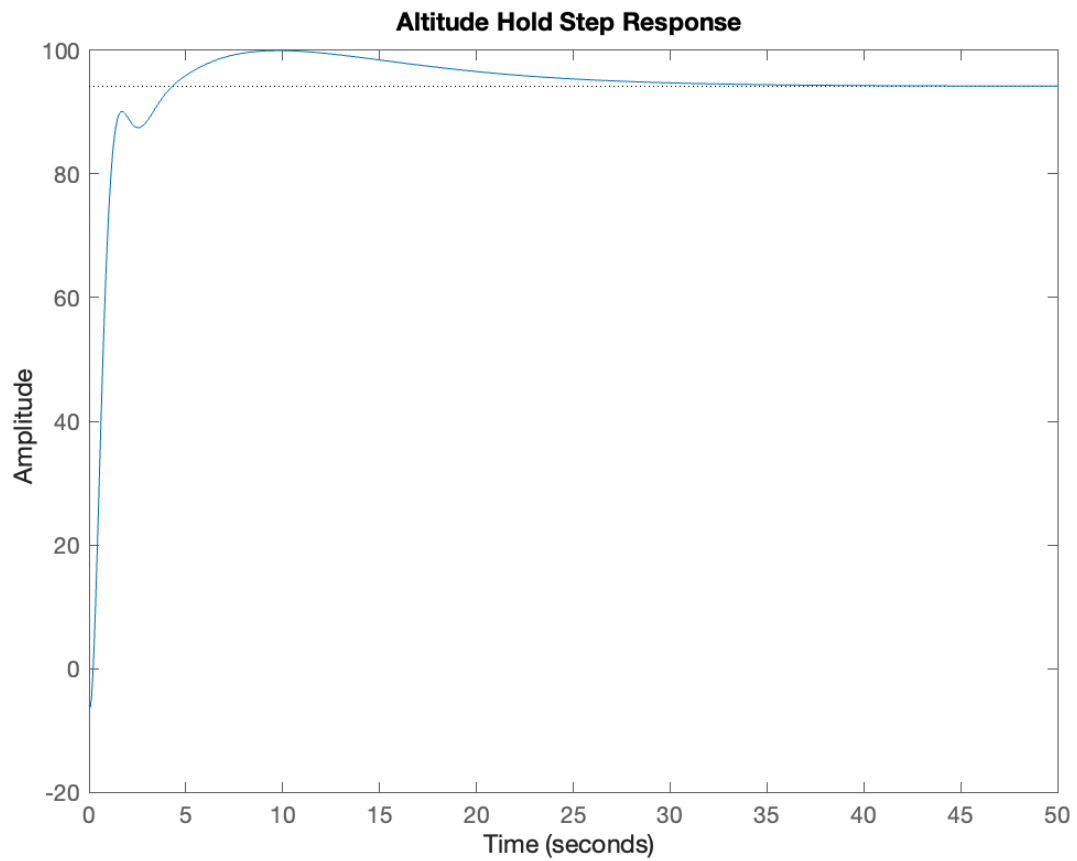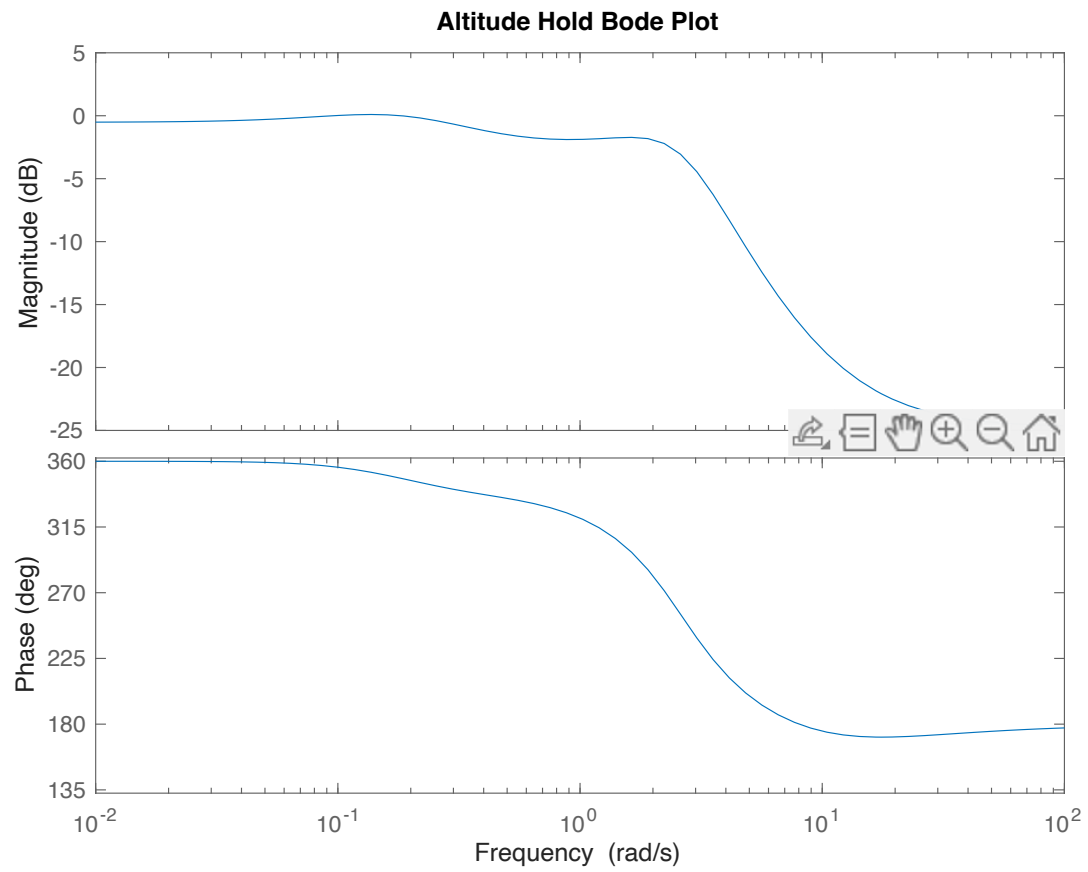
The graphs represent the step response and the Bode plot for the altitude hold control system of an aircraft, designed via a MATLAB simulation.

1. Altitude Hold Step Response:
The first graph displays the step response of the altitude hold system when subjected to a step input of 100 feet. Initially, the system experiences an overshoot, where the altitude momentarily exceeds the target by a significant margin, peaking at around 100 feet. This is followed by a rapid correction, bringing the amplitude down before settling. The system stabilizes close to the desired altitude within approximately 10 seconds, indicating effective damping and minimal steady-state error. This behavior shows the system's capability to regulate altitude changes swiftly and accurately, which is crucial for maintaining flight stability.

2. Altitude Hold Bode Plot:
The second graph shows the Bode plot of the same altitude hold system, displaying the frequency response across a range of frequencies. The magnitude plot (top) indicates a mild gain across low frequencies, peaking just below 0 dB, which starts to roll off significantly as the frequency increases. This suggests the system effectively attenuates higher frequency disturbances, beneficial for maintaining smooth altitude control. The phase plot (bottom) demonstrates a phase decrease with increasing frequency. The phase starts near 270 degrees and gradually trends downward, indicative of the system's time delay characteristics and the nature of the control strategy involving feedback and compensatory elements.

Together, these graphs provide crucial insights into the dynamics and performance of the altitude hold autopilot system, showcasing its effectiveness in maintaining target altitudes against disturbances while ensuring system stability and responsiveness.

Heading hold

The Matlab code is given in the appendix

Bode Plot for Heading Control System

Heading Hold Step Response: Degrees vs Time
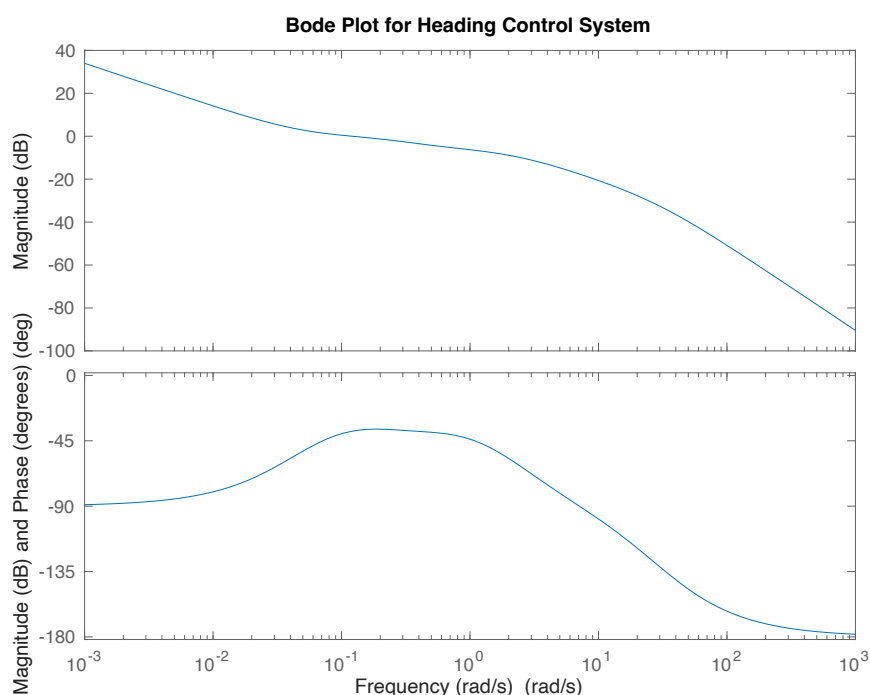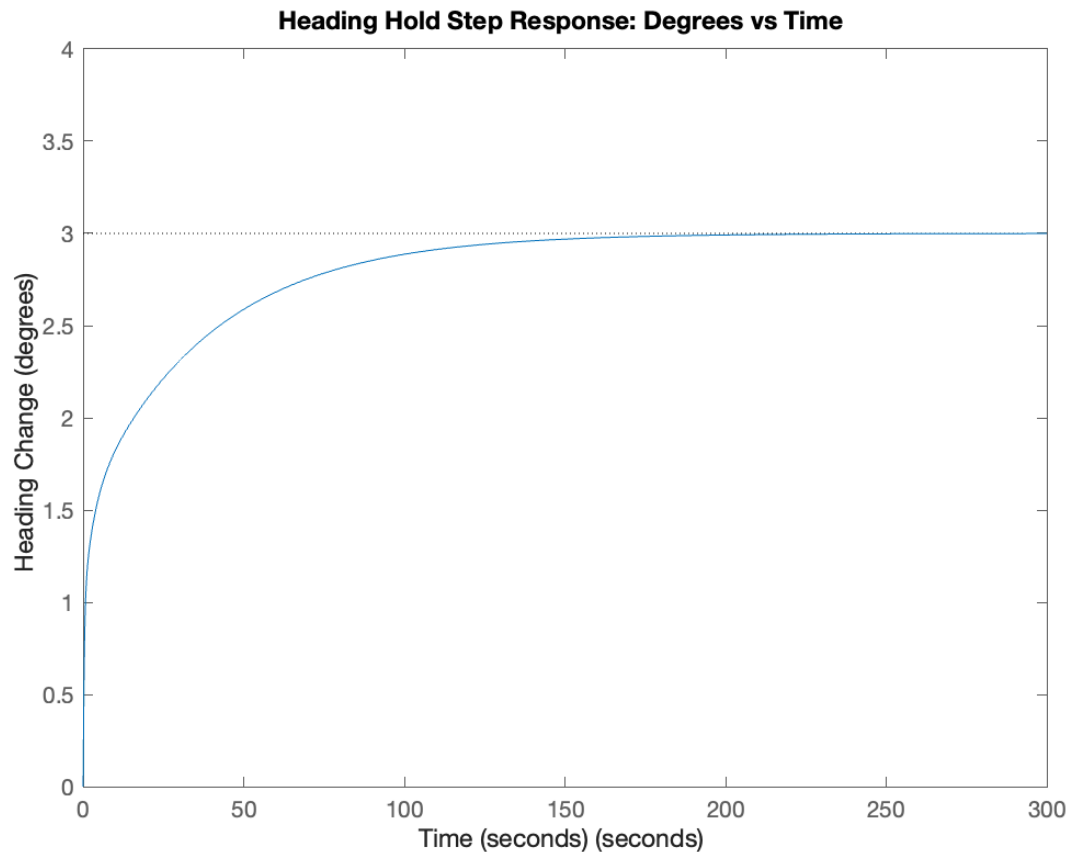
The images you've provided depict both the step response and the Bode plot for a heading control system.

Heading Hold Step Response: Degrees vs Time

- Graph Description: This graph shows the step response of a heading control system when subjected to a step change in desired heading. The response curve illustrates how the system's heading changes over time after the step input is applied.

-Observations: The system gradually increases its heading angle from 0 degrees, reaching near the target heading change of 3 degrees within approximately 50 seconds. After reaching the target, the heading changes slightly overshoots, stabilizing just above 3 degrees. The response is smooth and shows no oscillatory behavior, indicating a well-damped system. However, the rise time to the steady-state value is relatively slow, suggesting that the system might be tuned for high stability at the expense of response speed.

Bode Plot for Heading Control System
- Graph Description: This graph presents the Bode plot, showing the frequency response of the heading control system. It includes two subplots; the top shows the magnitude (in dB) and the bottom shows the phase (in degrees) across a range of frequencies.
- Observations:
    - Magnitude Plot: The magnitude decreases as the frequency increases, indicating that the system attenuates higher frequency inputs. This is typical for

systems designed to suppress noise and disturbances which often reside in higher frequency bands.

    - <u>Phase Plot</u>: The phase starts near 0 degrees at low frequencies and dips significantly as the frequency increases, crossing through -90 degrees. This typical phase behaviour suggests a system with lag characteristics, where the phase lag increases with frequency.

<u>Summary and Implications</u>

- <u>Step Response</u>: The extended response time in the step response graph could be indicative of a system that prioritizes stability and robustness over speed, which might be preferred in applications requiring precise heading control under varying conditions.

- <u>Bode Plot</u>: The Bode plot characteristics reinforce the system's capability to handle lower-frequency disturbances effectively while filtering out higher-frequency noise. The significant phase lag at higher frequencies might impact the system's ability to react swiftly to rapid changes, aligning with the observed slow response in the step response graph.

These observations are crucial for further tuning and potential adjustments in the system's design to balance responsiveness with stability, depending on specific operational requirements.

Part 2

The Matlab code is given in the Appendix.

This MATLAB code implements and simulates a Linear Quadratic Regulator (LQR) control strategy for a state-space model of a dynamic system, comparing the closed-loop (with feedback control) and open-loop (without feedback control) responses over a specified time period.

Key Components of the Code:

1. System Matrices Definition:
   - A: State transition matrix, defining how the states evolve without control input.
   - B: Control input matrix, defining how the control inputs affect the states.
   - Q: State weighting matrix in the LQR cost function, emphasizing the importance of certain states in the control strategy.
   - R: Control input weighting matrix in the LQR cost function, balancing the effort of the control inputs.

2. LQR Controller Design:
   - The `lqr` function is used to compute the optimal gain matrix K that minimizes the quadratic cost function, balancing the state deviations and control efforts.

3. Closed-Loop System Configuration: - The system matrix is adjusted (`A - B*K`) to incorporate the feedback mechanism via the LQR gain, forming the closed-loop system dynamics.

4. Open-Loop System Configuration: - The system is also set up in an open-loop configuration for comparison, where the system dynamics are purely based on the matrix **A** without any feedback control.

5.Simulation: - A time vector `t` is defined for simulation from 0 to 10 seconds.
   - Initial conditions X0 and zero input **u** are specified, reflecting no external disturbances.
   - The `lsim` function simulates both the closed-loop and open-loop systems, calculating the system outputs, states, and time vectors.

6. Plotting: - The responses, particularly the pitch rate (fourth state variable), are plotted to visualize the effect of the LQR control in stabilizing the system compared to the open-loop scenario.
   - Graphical features such as line types, colors, labels, and legends are used to enhance the readability and distinguish between the closed-loop and open-loop responses.

Overall, this script is a comprehensive implementation and analysis tool for assessing the effectiveness of LQR feedback control in dynamic systems, specifically monitoring the pitch rate behavior under different control configurations.

Comparison of Pitch Rate With and Without Feedback Control
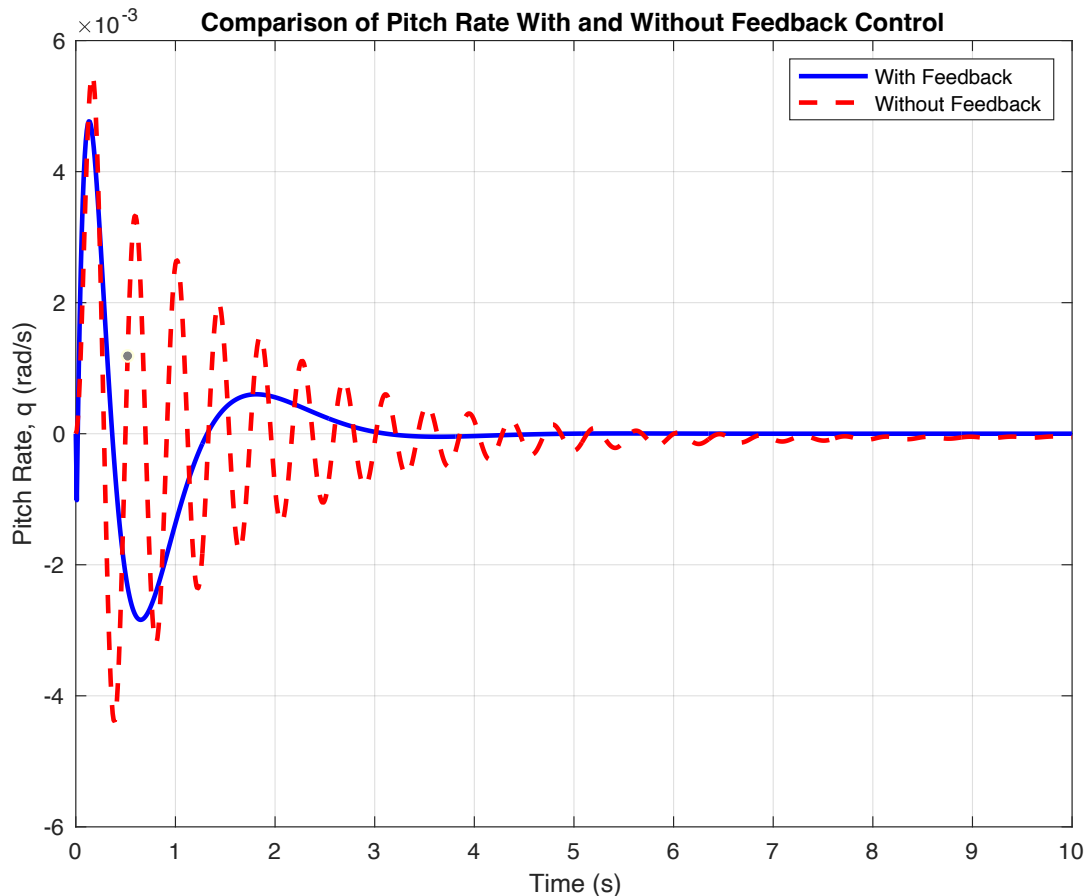
The graph displays a comparison of the pitch rate (in radians per second) over time (in seconds) for a dynamic system under two different control scenarios: with feedback control (shown as a solid blue line) and without feedback control (shown as a dashed red line).

Here's a detailed interpretation of the graph:

1. Initial Behavior (0 to about 2 seconds):
    - Both the controlled (with feedback) and uncontrolled (without feedback) responses start from the same initial condition. The pitch rate for both scenarios initially peaks sharply.
    - The system without feedback shows a more pronounced peak, reaching a higher maximum before beginning to oscillate.
    - The system with feedback control quickly reduces the amplitude of oscillation, showing a steeper decline after the initial peak.

2. Oscillation Behavior (2 to 10 seconds):
    - The uncontrolled system exhibits sustained and large amplitude oscillations throughout the simulation period, indicating instability or poor damping without feedback.
    - In contrast, the controlled system demonstrates rapidly diminishing oscillations, stabilizing to a steady state much faster than the uncontrolled system. This indicates effective damping and stabilization due to the LQR controller.

3. Settling Time: - The controlled system appears to settle near zero radians per second around 5 seconds into the simulation, showing effectiveness in achieving stability.
        - The uncontrolled system does not settle but continues to oscillate, demonstrating the critical role of the feedback control in stabilizing the pitch dynamics.

4. Overall Comparison: - The graph effectively illustrates the advantages of using feedback control in terms of response time to disturbances, stability, and oscillation damping.
        -The difference in response between the two scenarios underscores the effectiveness of the LQR control strategy implemented in the controlled system.

This visualization is particularly useful for understanding how feedback influences the dynamic behavior of a system, especially in critical applications such as aerospace engineering, where pitch control is crucial for the stability and performance of an aircraft.

Conclusion and Future Developments

Conclusion

This project presented an in-depth exploration of control systems in aerospace vehicles, focusing on the design and analysis of a selected aircraft not covered in our textbook appendices. Through detailed estimation, modeling, and simulation, I successfully developed state space models, designed effective control systems including pitch and yaw dampers, and created autopilots for altitude and heading hold.

Project Synthesis:
The initial phase of the project involved selecting an appropriate aircraft and estimating its stability derivatives using a combination of software tools and engineering judgment. This step was crucial as it laid the groundwork for the modeling and control designs that followed. The development of longitudinal and lateral state space models allowed for simulating responses to control inputs such as elevator and aileron movements, which was essential for understanding the aircraft's behavior under various flight conditions.

The design and implementation of pitch and yaw dampers were critical to enhancing the aircraft's stability by mitigating oscillatory modes such as the short-period pitch and the Dutch roll. These dampers significantly improved the aircraft's response to disturbances and maintained stability during flight operations.

For the advanced segment of the project, specifically aimed at ME 454 requirements, I delved into aeroelasticity by defining a bending mode along the longitudinal axis and examining its impact on the aircraft's aeroelastic stability. The solution involved designing a damper using the elevator to reduce vibrations associated with this bending mode, demonstrating an advanced application of control theory in aerospace engineering.

Autopilots Design:
The project culminated in the design of autopilots for altitude and heading maintenance. The effectiveness of these systems was validated through simulations showing the aircraft's dynamics in response to step changes in altitude and heading. These autopilots are integral to modern aviation, ensuring flight comfort and safety by maintaining stable flight conditions amidst various perturbations.

Intended Future Developments

Enhanced Modeling Techniques:
I plan to integrate more sophisticated modelling techniques that include machine learning algorithms to adaptively predict and respond to changing environmental conditions. This will enhance the robustness of the stability derivatives estimation and improve the overall predictive accuracy of the models.

Advanced Control Systems:
Further work will involve exploring adaptive control systems to enhance the adaptability of control designs to varying operational and environmental conditions. This includes developing more sophisticated autopilot systems capable of executing complex maneuvers and managing emergency situations.

Integration with Emerging Technologies:
The integration of emerging technologies such as unmanned aerial vehicles (UAVs) and electric propulsion systems will also be considered. Adjusting our existing models and control strategies to accommodate the unique characteristics of these technologies will be a key focus.

Collaborative and Real-Time Data Utilization:
I will also explore the potential for real-time data analytics and collaborative control systems, where multiple aircraft could share information to optimize flight paths and airspace management, leveraging advancements in communication technologies and data analytics.

Focus on Sustainability:
With environmental sustainability becoming increasingly important, future developments will aim to optimize control systems for better fuel efficiency and reduced environmental impacts. This includes potential studies on hybrid propulsion systems and optimizing flight trajectories for lower emissions.

In conclusion, this project has established a robust foundation for advancing aerospace vehicle control research. The methodologies and insights gained provide a valuable basis for tackling more complex aerospace challenges and integrating cutting-edge technologies in future work.

Appendix A

Following is the AVL Code for the project but the Geometry is too complex for Avl to Handle, So I mostly used XFLR5

```
F22 Raptor
0.0                      | Mach
0   0    0.0             | iYsym  iZsym  Zsym
 66.11715    5.56699   13.30000  | Sref  Cref  Bref
  5.94678    0.00000    0.25575  | Xref  Yref  Zref
 0.00                    | CDp  (optional)



SURFACE                | (keyword)
Main Wing
#Nchord    Cspace   [ Nspan Sspace ]
11       1.0

INDEX                  | (keyword)
7659                   | Lsurf

YDUPLICATE
0.0

SCALE
1.0  1.0  1.0

TRANSLATE
0.0  0.0  0.0

ANGLE
  0.000                | dAinc



#____PANEL 1_____
#_____
SECTION                              | (keyword)
  0.0000   0.0000   0.0000   7.6000   0.000   2   1  | Xle Yle Zle   Chord Ainc   [ Nspan
Sspace ]

AFIL 0.0 1.0
NACA 2412.dat



#_____
SECTION                              | (keyword)
  1.9000   2.0900   0.0000   5.7000   0.000   2   1  | Xle Yle Zle   Chord Ainc   [ Nspan
Sspace ]

AFIL 0.0 1.0
```

NACA 2412.dat

#____PANEL 2_____
#_____
SECTION | (keyword)
  1.9000   2.0900   0.0000   5.7000   0.000   2   1 | Xle Yle Zle   Chord Ainc   [Nspan Sspace]

AFIL 0.0 1.0
NACA 2412 straight with Flaps.dat

CONTROL | (keyword)
Main_Wing_Flap_1 1.0   0.750   0.7912   0.6115   0.0045 -1.0 | name, gain, Xhinge, XYZhvec, SgnDup

#_____
SECTION | (keyword)
  2.6500   2.9450   0.0000   6.1750   0.000   2   1 | Xle Yle Zle   Chord Ainc   [Nspan Sspace]

AFIL 0.0 1.0
NACA 2412 straight with Flaps.dat

CONTROL | (keyword)
Main_Wing_Flap_1 1.0   0.750   0.7912   0.6115   0.0045 -1.0 | name, gain, Xhinge, XYZhvec, SgnDup

#____PANEL 3_____
#_____
SECTION | (keyword)
  2.6500   2.9450   0.0000   6.1750   0.000   2   1 | Xle Yle Zle   Chord Ainc   [Nspan Sspace]

AFIL 0.0 1.0
NACA 2412 straight with Flaps.dat

CONTROL | (keyword)
Main_Wing_Flap_2 1.0   0.750   -0.0761   0.9970   -0.0167 -1.0 | name, gain, Xhinge, XYZhvec, SgnDup

#_____
SECTION | (keyword)
  3.8950   4.3700   0.0000   4.3700   0.000   2   1 | Xle Yle Zle   Chord Ainc   [Nspan Sspace]

AFIL 0.0 1.0
NACA 2412 straight with Flaps.dat

CONTROL | (keyword)

Main_Wing_Flap_2 1.0   0.750   -0.0761   0.9970   -0.0167 -1.0 | name, gain,
Xhinge, XYZhvec, SgnDup

#____PANEL 4_____
#_____
SECTION | (keyword)
  3.8950   4.3700   0.0000   4.3700   0.000   2   1 | Xle Yle Zle   Chord Ainc   [Nspan
Sspace]

AFIL 0.0 1.0
NACA 2412 straight with Flaps.dat

CONTROL | (keyword)
Main_Wing_Flap_3 1.0   0.750   -0.0460   0.9988   -0.0165 -1.0 | name, gain,
Xhinge, XYZhvec, SgnDup

#_____
SECTION | (keyword)
  5.2500   5.8900   0.0000   2.4700   0.000   2   1 | Xle Yle Zle   Chord Ainc   [Nspan
Sspace]

AFIL 0.0 1.0
NACA 2412 straight with Flaps.dat

CONTROL | (keyword)
Main_Wing_Flap_3 1.0   0.750   -0.0460   0.9988   -0.0165 -1.0 | name, gain,
Xhinge, XYZhvec, SgnDup

#____PANEL 5_____
#_____
SECTION | (keyword)
  5.2500   5.8900   0.0000   2.4700   0.000   3   1 | Xle Yle Zle   Chord Ainc   [Nspan
Sspace]

AFIL 0.0 1.0
NACA 2412 straight with Flaps.dat

CONTROL | (keyword)
Main_Wing_Flap_4 1.0   0.750   -0.4256   0.9047   -0.0209 -1.0 | name, gain,
Xhinge, XYZhvec, SgnDup

#_____
SECTION | (keyword)
  5.8900   6.6500   0.0000   1.1400   0.000   3   1 | Xle Yle Zle   Chord Ainc   [Nspan
Sspace]

AFIL 0.0 1.0
NACA 2412 straight with Flaps.dat

CONTROL | (keyword)

Main_Wing_Flap_4 1.0   0.750   -0.4256   0.9047   -0.0209 -1.0 | name, gain, Xhinge, XYZhvec, SgnDup

SURFACE | (keyword)
Elevator
#Nchord   Cspace   [Nspan Sspace]
7   1.0

INDEX | (keyword)
7661 | Lsurf

YDUPLICATE
0.0

SCALE
1.0 1.0 1.0

TRANSLATE
0.0 0.0 0.0

ANGLE
  0.000 | dAinc

#____PANEL 1_____
#_____
SECTION | (keyword)
  7.7000   0.0000   0.0000   2.0900   0.000   10   1 | Xle Yle Zle   Chord Ainc   [Nspan Sspace]

AFIL 0.0 1.0
NACA 2412.dat

#_____
SECTION | (keyword)
  7.7000   1.4000   0.0000   2.0900   0.000   10   1 | Xle Yle Zle   Chord Ainc   [Nspan Sspace]

AFIL 0.0 1.0
NACA 2412.dat

#____PANEL 2_____
#_____
SECTION | (keyword)
  7.7000   1.4000   0.0000   3.0400   0.000   2   1 | Xle Yle Zle   Chord Ainc   [Nspan Sspace]

```
AFIL 0.0 1.0
NACA 2412.dat


#_____
SECTION                              | (keyword)
  7.7000   1.9950   0.0000   3.5000   0.000   2   1  | Xle Yle Zle   Chord Ainc   [ Nspan
Sspace ]

AFIL 0.0 1.0
NACA 2412.dat


#_____PANEL 3_____
#_____
SECTION                              | (keyword)
  7.7000   1.9950   0.0000   3.5000   0.000   2   1  | Xle Yle Zle   Chord Ainc   [ Nspan
Sspace ]

AFIL 0.0 1.0
NACA 2412 straight with Flaps Elevator.dat

CONTROL                              | (keyword)
Elevator_Flap_1 1.0   0.500      0.6692      0.7431     -0.0078 -1.0 | name, gain,  Xhinge,
XYZhvec,  SgnDup


#_____
SECTION                              | (keyword)
  8.7000   2.8500   0.0000   3.0400   0.000   2   1  | Xle Yle Zle   Chord Ainc   [ Nspan
Sspace ]

AFIL 0.0 1.0
NACA 2412 straight with Flaps Elevator.dat

CONTROL                              | (keyword)
Elevator_Flap_1 1.0   0.500      0.6692      0.7431     -0.0078 -1.0 | name, gain,  Xhinge,
XYZhvec,  SgnDup


#_____PANEL 4_____
#_____
SECTION                              | (keyword)
  8.7000   2.8500   0.0000   3.0400   0.000   2   1  | Xle Yle Zle   Chord Ainc   [ Nspan
Sspace ]

AFIL 0.0 1.0
NACA 2412 straight with Flaps Elevator.dat

CONTROL                              | (keyword)
Elevator_Flap_2 1.0   0.500      0.4679      0.8836     -0.0193 -1.0 | name, gain,  Xhinge,
XYZhvec,  SgnDup
```

#_____
SECTION | (keyword)
  10.3600   4.3700   0.0000   1.3300   0.000   2   1 | Xle Yle Zle   Chord Ainc   [Nspan Sspace]

AFIL 0.0 1.0
NACA 2412 straight with Flaps Elevator.dat

CONTROL | (keyword)
Elevator_Flap_2 1.0   0.500   0.4679   0.8836   -0.0193 -1.0 | name, gain, Xhinge, XYZhvec, SgnDup

SURFACE | (keyword)
Fin
#Nchord   Cspace   [Nspan Sspace]
7   1.0

INDEX | (keyword)
7662 | Lsurf

YDUPLICATE
  0.0000

SCALE
1.0 1.0 1.0

TRANSLATE
0.0 0.0 0.0

ANGLE
  0.000 | dAinc

#____PANEL 1_____
#_____
SECTION | (keyword)
  6.4000   -3.2943   3.2766   1.2000   0.000   5   0 | Xle Yle Zle   Chord Ainc   [Nspan Sspace]

AFIL 0.0 1.0
NACA 2412 straight with Flaps Fin.dat

CONTROL | (keyword)
Fin_Flap_1 1.0   0.700   0.2055   0.5709   -0.7949 -1.0 | name, gain, Xhinge, XYZhvec, SgnDup

#_____
SECTION | (keyword)

```
   5.7000   -2.1472   1.6383   2.8000   0.000   5   0  | Xle Yle Zle   Chord Ainc   [ Nspan
Sspace ]

AFIL 0.0 1.0
NACA 2412 straight with Flaps Fin.dat

CONTROL                                    |  (keyword)
Fin_Flap_1  1.0   0.700        0.2055        0.5709      -0.7949  -1.0  | name, gain,  Xhinge,
XYZhvec,  SgnDup


#____PANEL 2_____
#_____
SECTION                                    |  (keyword)
   5.7000   -2.1472   1.6383   2.8000   0.000   5   0  | Xle Yle Zle   Chord Ainc   [ Nspan
Sspace ]

AFIL 0.0 1.0
NACA 2412 straight with Flaps Fin.dat

CONTROL                                    |  (keyword)
Fin_Flap_2  1.0   0.700        0.2055        0.5709      -0.7949  -1.0  | name, gain,  Xhinge,
XYZhvec,  SgnDup


#_____
SECTION                                    |  (keyword)
   5.0000   -1.0000   0.0000   4.4000   0.000   5   0  | Xle Yle Zle   Chord Ainc   [ Nspan
Sspace ]

AFIL 0.0 1.0
NACA 2412 straight with Flaps Fin.dat

CONTROL                                    |  (keyword)
Fin_Flap_2  1.0   0.700        0.2055        0.5709      -0.7949  -1.0  | name, gain,  Xhinge,
XYZhvec,  SgnDup


#____PANEL 3_____
#_____
SECTION                                    |  (keyword)
   5.0000    1.0000   0.0000   4.4000   0.000   5   0  | Xle Yle Zle   Chord Ainc   [ Nspan
Sspace ]

AFIL 0.0 1.0
NACA 2412 straight with Flaps Fin.dat

CONTROL                                    |  (keyword)
Fin_Flap_3  1.0   0.700       -0.2055        0.5709       0.7949  -1.0  | name, gain,  Xhinge,
XYZhvec,  SgnDup


#_____
SECTION                                    |  (keyword)
```

```
    5.7000    2.1472    1.6383    2.8000    0.000    5    0   | Xle Yle Zle   Chord Ainc   [ Nspan
Sspace ]

AFIL 0.0 1.0
NACA 2412 straight with Flaps Fin.dat

CONTROL                                        | (keyword)
Fin_Flap_3  1.0   0.700      -0.2055      0.5709      0.7949  -1.0  | name, gain,  Xhinge,
XYZhvec,  SgnDup


#_____PANEL 4_____
#_____
SECTION                                        | (keyword)
    5.7000    2.1472    1.6383    2.8000    0.000    5    0   | Xle Yle Zle   Chord Ainc   [ Nspan
Sspace ]

AFIL 0.0 1.0
NACA 2412 straight with Flaps Fin.dat

CONTROL                                        | (keyword)
Fin_Flap_4  1.0   0.700      -0.2055      0.5709      0.7949  -1.0  | name, gain,  Xhinge,
XYZhvec,  SgnDup


#_____
SECTION                                        | (keyword)
    6.4000    3.2943    3.2766    1.2000    0.000    5    0   | Xle Yle Zle   Chord Ainc   [ Nspan
Sspace ]

AFIL 0.0 1.0
NACA 2412 straight with Flaps Fin.dat

CONTROL                                        | (keyword)
Fin_Flap_4  1.0   0.700      -0.2055      0.5709      0.7949  -1.0  | name, gain,  Xhinge,
XYZhvec,  SgnDup
```

Appendix B

Adding all the polar analysis data will take around 720 pages of the report, so I will add a few of them for example of the analysis.

xflr5 v6.61

 Calculated polar for: NACA 2412

 1 1 Reynolds number fixed   Mach number fixed

 xtrf =   1.000 (top)   1.000 (bottom)
 Mach =   0.000   Re =   0.030 e 6   Ncrit =   9.000

alpha	CL	CD	CDp	Cm	Top Xtr	Bot Xtr	Cpmin	Chinge	XCp
-10.000	-0.3952	0.12477	0.11479	0.0029	1.0000	0.4665	-1.2249	0.0000	0.0000 0.0000 0.2456
-9.500	-0.4099	0.12368	0.11383	0.0062	1.0000	0.5072	-1.2437	0.0000	0.0000 0.0000 0.2544
-9.000	-0.3595	0.11118	0.10119	0.0047	1.0000	0.5486	-1.1557	0.0000	0.0000 0.0000 0.2516
-8.500	-0.3515	0.10640	0.09646	0.0068	1.0000	0.5920	-1.1610	0.0000	0.0000 0.0000 0.2582
-8.000	-0.3176	0.09809	0.08813	0.0069	1.0000	0.6482	-1.1302	0.0000	0.0000 0.0000 0.2602
-7.500	-0.2857	0.09001	0.08004	0.0062	1.0000	0.6963	-1.1006	0.0000	0.0000 0.0000 0.2595
-7.000	-0.2875	0.08475	0.07488	0.0066	1.0000	0.6907	-1.1193	0.0000	0.0000 0.0000 0.2618
-6.500	-0.5175	0.06738	0.05834	-0.0236	1.0000	0.2730	-1.9034	0.0000	0.0000 0.0000 0.1988
-6.000	-0.5219	0.05896	0.04973	-0.0239	1.0000	0.2751	-1.9657	0.0000	0.0000 0.0000 0.1989
-5.500	-0.5140	0.05132	0.04159	-0.0240	1.0000	0.2864	-1.9950	0.0000	0.0000 0.0000 0.1982
-5.000	-0.4882	0.04470	0.03447	-0.0229	1.0000	0.3003	-1.9550	0.0000	0.0000 0.0000 0.1982
-4.500	-0.4565	0.03995	0.02931	-0.0210	1.0000	0.3362	-1.8683	0.0000	0.0000 0.0000 0.1991
-4.000	-0.4186	0.03589	0.02507	-0.0187	1.0000	0.3828	-1.7469	0.0000	0.0000 0.0000 0.2006
-3.500	-0.3792	0.03259	0.02163	-0.0160	1.0000	0.4527	-1.6101	0.0000	0.0000 0.0000 0.2031
-3.000	-0.3433	0.03022	0.01965	-0.0105	1.0000	0.5516	-1.4850	0.0000	0.0000 0.0000 0.2147
-2.500	-0.3169	0.02833	0.01839	-0.0013	1.0000	0.6947	-1.3690	0.0000	0.0000 0.0000 0.2414
-2.000	-0.1237	0.02640	0.01573	-0.0249	1.0000	1.0000	-0.9913	0.0000	0.0000 0.0000 0.0398

-1.500	-0.1365	0.02577	0.01460	-0.0187	1.0000	1.0000	-0.9533	0.0000	0.0000	0.0000	0.1062
-1.000	-0.1157	0.02611	0.01437	-0.0162	1.0000	1.0000	-0.8547	0.0000	0.0000	0.0000	0.1041
-0.500	-0.0873	0.02684	0.01464	-0.0147	1.0000	1.0000	-0.7520	0.0000	0.0000	0.0000	0.0766
0.000	-0.0565	0.02786	0.01524	-0.0137	1.0000	1.0000	-0.6557	0.0000	0.0000	0.0000	0.0033
0.500	-0.0249	0.02916	0.01623	-0.0132	1.0000	1.0000	-0.5674	0.0000	0.0000	0.0000	-0.2790
1.000	0.0068	0.03071	0.01755	-0.0130	1.0000	1.0000	-0.4871	0.0000	0.0000	0.0000	2.1220
1.500	0.0385	0.03252	0.01917	-0.0131	1.0000	1.0000	-0.4383	0.0000	0.0000	0.0000	0.5797
2.000	0.0699	0.03456	0.02109	-0.0135	1.0000	1.0000	-0.4614	0.0000	0.0000	0.0000	0.4339
2.500	0.1009	0.03685	0.02328	-0.0142	1.0000	1.0000	-0.4859	0.0000	0.0000	0.0000	0.3811
3.000	0.1444	0.03982	0.02620	-0.0175	0.9940	1.0000	-0.5214	0.0000	0.0000	0.0000	0.3626
3.500	0.2362	0.04436	0.03079	-0.0297	0.9530	1.0000	-0.5979	0.0000	0.0000	0.0000	0.3684
4.000	0.3093	0.04840	0.03495	-0.0376	0.9134	1.0000	-0.6743	0.0000	0.0000	0.0000	0.3646
4.500	0.3820	0.05255	0.03930	-0.0446	0.8726	1.0000	-0.7675	0.0000	0.0000	0.0000	0.3599
5.000	0.4348	0.05628	0.04322	-0.0480	0.8326	1.0000	-0.8578	0.0000	0.0000	0.0000	0.3534
5.500	0.4895	0.06033	0.04749	-0.0511	0.7907	1.0000	-0.9673	0.0000	0.0000	0.0000	0.3472
6.000	0.5532	0.06430	0.05186	-0.0543	0.7440	1.0000	-1.1106	0.0000	0.0000	0.0000	0.3408
6.500	0.5791	0.06857	0.05633	-0.0533	0.7021	1.0000	-1.1975	0.0000	0.0000	0.0000	0.3343
7.000	0.6361	0.07251	0.06061	-0.0538	0.6496	1.0000	-1.3625	0.0000	0.0000	0.0000	0.3267
7.500	0.6913	0.07597	0.06444	-0.0526	0.5931	1.0000	-1.5367	0.0000	0.0000	0.0000	0.3179
8.000	0.6939	0.08165	0.07029	-0.0501	0.5493	1.0000	-1.5770	0.0000	0.0000	0.0000	0.3135
8.500	0.7247	0.08637	0.07539	-0.0474	0.4964	1.0000	-1.7065	0.0000	0.0000	0.0000	0.3064
9.000	0.7574	0.09092	0.08020	-0.0441	0.4439	1.0000	-1.8407	0.0000	0.0000	0.0000	0.2988
9.500	0.7527	0.09890	0.08826	-0.0433	0.4104	1.0000	-1.8397	0.0000	0.0000	0.0000	0.2976
10.000	0.7518	0.10726	0.09670	-0.0432	0.3826	1.0000	-1.8364	0.0000	0.0000	0.0000	0.2970

xflr5 v6.61

Calculated polar for: NACA 2412 straight with Flaps Fin

1 1 Reynolds number fixed   Mach number fixed

xtrf =   1.000 (top)   1.000 (bottom)
Mach =   0.000   Re =   0.130 e 6   Ncrit =   9.000

alpha,CL,CD,CDp,Cm,Top Xtr,Bot Xtr,Cpmin,Chinge,XCp
-10.000,-0.4677, 0.10472, 0.09996,-0.0243,1.0000,0.1147,-1.7593,-0.0010, 0.0000,
0.0000, 0.1876
  -9.500,-0.5177, 0.09234, 0.08779,-0.0375,1.0000,0.1208,-2.1007,-0.0004, 0.0000,
0.0000, 0.1684
  -9.000,-0.4899, 0.08650, 0.08194,-0.0335,1.0000,0.1237,-1.9558,-0.0004, 0.0000,
0.0000, 0.1726
  -8.500,-0.5026, 0.07798, 0.07354,-0.0366,1.0000,0.1259,-2.0267,-0.0001, 0.0000,
0.0000, 0.1690
  -8.000,-0.6868, 0.03885, 0.03255,-0.0424,1.0000,0.0666,-3.5806,-0.0022, 0.0000,
0.0000, 0.1801
  -7.500,-0.6725, 0.03314, 0.02602,-0.0376,1.0000,0.0690,-3.5397,-0.0028, 0.0000,
0.0000, 0.1862
  -7.000,-0.6449, 0.02957, 0.02160,-0.0336,1.0000,0.0725,-3.4019,-0.0031, 0.0000,
0.0000, 0.1904
  -6.500,-0.6103, 0.02639, 0.01830,-0.0312,1.0000,0.0801,-3.1524,-0.0031, 0.0000,
0.0000, 0.1917
  -6.000,-0.5712, 0.02398, 0.01543,-0.0287,1.0000,0.0887,-2.9238,-0.0031, 0.0000,
0.0000, 0.1928
  -5.500,-0.5292, 0.02215, 0.01354,-0.0268,1.0000,0.0989,-2.6997,-0.0030, 0.0000,
0.0000, 0.1927
  -5.000,-0.4854, 0.02067, 0.01202,-0.0253,1.0000,0.1140,-2.4849,-0.0028, 0.0000,
0.0000, 0.1914
  -4.500,-0.4411, 0.01951, 0.01079,-0.0239,1.0000,0.1342,-2.2634,-0.0025, 0.0000,
0.0000, 0.1894
  -4.000,-0.3961, 0.01846, 0.00989,-0.0230,0.9998,0.1629,-2.0387,-0.0021, 0.0000,
0.0000, 0.1857
  -3.500,-0.3094, 0.01749, 0.00923,-0.0301,0.9874,0.2259,-1.7125,-0.0001, 0.0000,
0.0000, 0.1461
  -3.000,-0.2266, 0.01662, 0.00885,-0.0364,0.9734,0.3235,-1.4449, 0.0016, 0.0000,
0.0000, 0.0819
  -2.500,-0.1474, 0.01565, 0.00858,-0.0417,0.9582,0.4691,-1.1914, 0.0032, 0.0000,
0.0000,-0.0419
  -2.000,-0.0698, 0.01472, 0.00860,-0.0452,0.9438,0.6866,-0.9673, 0.0048, 0.0000,
0.0000,-0.4127
  -1.500,-0.0009, 0.01439, 0.00875,-0.0452,0.9264,0.8607,-0.7798, 0.0044, 0.0000,
0.0000,-52.0106
  -1.000, 0.1092, 0.01443, 0.00868,-0.0538,0.9140,0.9617,-0.5713, 0.0054, 0.0000,
0.0000, 0.7464
    0.000, 0.3260, 0.01329, 0.00718,-0.0738,0.8784,1.0000,-0.6066, 0.0090, 0.0000,
0.0000, 0.4755
    0.500, 0.3731, 0.01297, 0.00671,-0.0717,0.8451,1.0000,-0.6525, 0.0083, 0.0000,
0.0000, 0.4405

1.000, 0.4199, 0.01279, 0.00637,-0.0693,0.8107,1.0000,-0.7028, 0.0077, 0.0000, 0.0000, 0.4128

1.500, 0.4679, 0.01272, 0.00613,-0.0670,0.7772,1.0000,-0.7610, 0.0071, 0.0000, 0.0000, 0.3905

2.000, 0.5165, 0.01280, 0.00604,-0.0649,0.7442,1.0000,-0.8292, 0.0068, 0.0000, 0.0000, 0.3724

2.500, 0.5644, 0.01303, 0.00609,-0.0627,0.7106,1.0000,-0.9131, 0.0067, 0.0000, 0.0000, 0.3575

3.000, 0.6116, 0.01332, 0.00626,-0.0606,0.6780,1.0000,-1.0189, 0.0066, 0.0000, 0.0000, 0.3449

3.500, 0.6590, 0.01372, 0.00655,-0.0585,0.6443,1.0000,-1.1483, 0.0067, 0.0000, 0.0000, 0.3342

4.000, 0.7066, 0.01413, 0.00692,-0.0564,0.6106,1.0000,-1.3018, 0.0068, 0.0000, 0.0000, 0.3249

4.500, 0.7542, 0.01455, 0.00724,-0.0543,0.5762,1.0000,-1.4753, 0.0070, 0.0000, 0.0000, 0.3166

5.000, 0.8019, 0.01500, 0.00755,-0.0523,0.5402,1.0000,-1.6749, 0.0072, 0.0000, 0.0000, 0.3092

5.500, 0.8479, 0.01549, 0.00799,-0.0500,0.5014,1.0000,-1.8777, 0.0072, 0.0000, 0.0000, 0.3025

6.000, 0.8925, 0.01596, 0.00847,-0.0476,0.4587,1.0000,-2.1212, 0.0073, 0.0000, 0.0000, 0.2963

6.500, 0.9355, 0.01652, 0.00898,-0.0450,0.4114,1.0000,-2.3672, 0.0072, 0.0000, 0.0000, 0.2905

7.000, 0.9753, 0.01721, 0.00957,-0.0419,0.3549,1.0000,-2.6119, 0.0071, 0.0000, 0.0000, 0.2848

7.500, 1.0098, 0.01834, 0.01042,-0.0383,0.2857,1.0000,-2.8458, 0.0068, 0.0000, 0.0000, 0.2792

8.000, 1.0381, 0.02016, 0.01190,-0.0341,0.2093,1.0000,-3.0994, 0.0065, 0.0000, 0.0000, 0.2735

8.500, 1.0618, 0.02258, 0.01389,-0.0296,0.1533,1.0000,-3.3335, 0.0061, 0.0000, 0.0000, 0.2678

9.000, 1.0867, 0.02509, 0.01617,-0.0254,0.1213,1.0000,-3.5667, 0.0059, 0.0000, 0.0000, 0.2627

9.500, 1.1152, 0.02781, 0.01881,-0.0217,0.1015,1.0000,-3.8030, 0.0058, 0.0000, 0.0000, 0.2582

10.000, 1.1447, 0.03050, 0.02151,-0.0186,0.0865,1.0000,-4.0495, 0.0057, 0.0000, 0.0000, 0.2542

xflr5 v6.61

Calculated polar for: NACA 2412 straight with Flaps Fin

3 1 Reynolds number ~ 1/CL   Mach number fixed

xtrf =   1.000 (top)   1.000 (bottom)
Mach =   0.000   Re =   1536.000 e 6   Ncrit =   9.000

alpha,CL,CD,CDp,Cm,Top Xtr,Bot Xtr,Cpmin,Chinge,XCp

-10.000,-0.9346, 0.00350, 0.00142,-0.0445,0.0363,0.0156,-6.8962,-0.0027, 0.0000, 0.0000, 0.1915
 -7.000,-0.5825, 0.00289, 0.00082,-0.0470,0.0239,0.0069,-3.8376,-0.0004, 0.0000, 0.0000, 0.1609
 -5.000,-0.3454, 0.00265, 0.00058,-0.0490,0.0121,0.0023,-2.3481, 0.0013, 0.0000, 0.0000, 0.1001
 -1.500, 0.0704, 0.00297, 0.00048,-0.0527,0.0069,0.0030,-0.6900, 0.0041, 0.0000, 0.0000, 1.0053
 -1.000, 0.1294, 0.00315, 0.00050,-0.0532,0.0121,0.0031,-0.5509, 0.0045, 0.0000, 0.0000, 0.6626
 -0.500, 0.1884, 0.00327, 0.00052,-0.0536,0.0123,0.0070,-0.5251, 0.0049, 0.0000, 0.0000, 0.5344
  0.000, 0.2473, 0.00337, 0.00054,-0.0541,0.0134,0.0121,-0.5718, 0.0053, 0.0000, 0.0000, 0.4674
  0.500, 0.3061, 0.00346, 0.00057,-0.0545,0.0121,0.0149,-0.6223, 0.0057, 0.0000, 0.0000, 0.4261
  1.000, 0.3649, 0.00356, 0.00060,-0.0550,0.0102,0.0158,-0.6778, 0.0061, 0.0000, 0.0000, 0.3981
  1.500, 0.4236, 0.00364, 0.00064,-0.0554,0.0098,0.0243,-0.7397, 0.0064, 0.0000, 0.0000, 0.3778
  2.000, 0.4822, 0.00373, 0.00068,-0.0559,0.0103,0.0250,-0.8115, 0.0068, 0.0000, 0.0000, 0.3624
  2.500, 0.5407, 0.00382, 0.00073,-0.0563,0.0106,0.0264,-0.9009, 0.0072, 0.0000, 0.0000, 0.3502
  3.000, 0.5991, 0.00391, 0.00078,-0.0567,0.0109,0.0385,-1.0182, 0.0075, 0.0000, 0.0000, 0.3404
  3.500, 0.6574, 0.00401, 0.00084,-0.0571,0.0102,0.0465,-1.1655, 0.0079, 0.0000, 0.0000, 0.3322
  4.000, 0.7153, 0.00413, 0.00093,-0.0575,0.0063,0.0470,-1.3431, 0.0082, 0.0000, 0.0000, 0.3252
  4.500, 0.7733, 0.00424, 0.00101,-0.0579,0.0063,0.0593,-1.5485, 0.0086, 0.0000, 0.0000, 0.3192
  5.000, 0.8311, 0.00436, 0.00110,-0.0582,0.0063,0.0600,-1.7730, 0.0089, 0.0000, 0.0000, 0.3140
  5.500, 0.8889, 0.00446, 0.00117,-0.0586,0.0068,0.0750,-2.0402, 0.0093, 0.0000, 0.0000, 0.3094
  6.000, 0.9464, 0.00459, 0.00127,-0.0589,0.0068,0.0760,-2.3262, 0.0096, 0.0000, 0.0000, 0.3052
  6.500, 1.0035, 0.00474, 0.00139,-0.0592,0.0065,0.0861,-2.6215, 0.0099, 0.0000, 0.0000, 0.3014
  7.000, 1.0602, 0.00492, 0.00154,-0.0594,0.0049,0.0996,-2.9556, 0.0102, 0.0000, 0.0000, 0.2978
  7.500, 1.1170, 0.00507, 0.00167,-0.0596,0.0052,0.1026,-3.3353, 0.0105, 0.0000, 0.0000, 0.2946
  8.500, 1.2296, 0.00542, 0.00198,-0.0600,0.0037,0.1300,-4.1391, 0.0111, 0.0000, 0.0000, 0.2887
  9.000, 1.2854, 0.00561, 0.00214,-0.0601,0.0030,0.1396,-4.5644, 0.0114, 0.0000, 0.0000, 0.2860
  9.500, 1.3410, 0.00581, 0.00231,-0.0602,0.0030,0.1523,-5.0058, 0.0116, 0.0000, 0.0000, 0.2834
 10.000, 1.3963, 0.00601, 0.00249,-0.0603,0.0030,0.1568,-5.4623, 0.0119, 0.0000, 0.0000, 0.2810

xflr5 v6.61

Calculated polar for: NACA 2412

3 1 Reynolds number ~ 1/CL   Mach number fixed

xtrf =   1.000 (top)   1.000 (bottom)
Mach =   0.000   Re = 24576.000 e 6   Ncrit =   9.000

alpha,CL,CD,CDp,Cm,Top Xtr,Bot Xtr,Cpmin,Chinge,XCp
  -0.500, 0.1904, 0.00252, 0.00041,-0.0541,0.0030,0.0008,-0.5265, 0.0000, 0.0000,
0.0000, 0.5337
    1.000, 0.3683, 0.00272, 0.00046,-0.0557,0.0008,0.0031,-0.6804, 0.0000, 0.0000,
0.0000, 0.3986
    3.500, 0.6632, 0.00306, 0.00066,-0.0583,0.0000,0.0121,-1.1747, 0.0000, 0.0000,
0.0000, 0.3331
    4.000, 0.7218, 0.00315, 0.00072,-0.0587,0.0000,0.0121,-1.3553, 0.0000, 0.0000,
0.0000, 0.3262
    5.000, 0.8387, 0.00333, 0.00085,-0.0597,0.0000,0.0188,-1.7936, 0.0000, 0.0000,
0.0000, 0.3151
    5.500, 0.8969, 0.00344, 0.00094,-0.0601,0.0006,0.0188,-2.0655, 0.0000, 0.0000,
0.0000, 0.3104
    6.000, 0.9549, 0.00355, 0.00103,-0.0605,0.0008,0.0207,-2.3544, 0.0000, 0.0000,
0.0000, 0.3063
    6.500, 1.0127, 0.00367, 0.00112,-0.0609,0.0008,0.0269,-2.6551, 0.0000, 0.0000,
0.0000, 0.3025
    7.000, 1.0703, 0.00379, 0.00123,-0.0613,0.0008,0.0269,-2.9943, 0.0000, 0.0000,
0.0000, 0.2991
    8.000, 1.1846, 0.00410, 0.00150,-0.0619,0.0009,0.0409,-3.7758, 0.0000, 0.0000,
0.0000, 0.2928
    8.500, 1.2415, 0.00424, 0.00163,-0.0622,0.0031,0.0470,-4.1914, 0.0000, 0.0000,
0.0000, 0.2900
    9.000, 1.2980, 0.00441, 0.00178,-0.0624,0.0018,0.0471,-4.6216, 0.0000, 0.0000,
0.0000, 0.2873
    9.500, 1.3543, 0.00459, 0.00194,-0.0627,0.0031,0.0591,-5.0682, 0.0000, 0.0000,
0.0000, 0.2848
   10.000, 1.4102, 0.00478, 0.00212,-0.0628,0.0031,0.0591,-5.5293, 0.0000, 0.0000,
0.0000, 0.2823

Appendix C

The formulae for the Calculation A and B matrices are taken from the textbook. In my context, XFLR5 calculates the state space models for us. We have to Decouple the state space system to get the Matrices A and B.

Table 6.2 Summary for Vehicle Lift, Drag, and Pitching Moment

	$\alpha = \delta_E = i_H = 0$ (plus $\beta = \delta_R = 0$ for drag)	Angle of Attack, α	Elevator Deflection, δ_E	Tail Incidence, i_H
Lift, C_L	$C_{L_{a_w}}(i_w - \alpha_{0_w}) +$ $C_{L_{a_H}}\overline{q}\overline{S}_H\left(\dfrac{d\varepsilon}{d\alpha}(\alpha_{0_w} - i_w) - \alpha_{0_H}\right)$ Equation (6.21)	$C_{L_{a_w}} + C_{L_{a_H}}\overline{q}\overline{S}_H\overline{\varepsilon}$ Equation (6.18)	$C_{L_{a_H}}\alpha_\delta \overline{q}\overline{S}_H$ $= C_{L_{\delta_H}}\overline{q}\overline{S}_H$ Equation (6.19)	$C_{L_{a_H}}\overline{q}\overline{S}_H$ Equation (6.20)
Drag, C_D	$C_{D_0} + \dfrac{1}{\pi A_w e_w}\left(C_{L_w}^2 + C_{L_H}^2 \dfrac{A_w e_w}{A_H e_H}\overline{q}\overline{S}_H\right)$ Equation (6.36)	$\dfrac{2C_{L_w}C_{L_{a_w}}}{\pi A_w e_w}\left(\dfrac{1 + \frac{C_{L_H}C_{L_{a_H}}}{C_{L_w}C_{L_{a_w}}}\frac{A_w e_w}{A_H e_H}\overline{q}\overline{S}_H\overline{\varepsilon}}{}\right)$ Equation (6.31)	$C_{L_{a_H}}\alpha_\delta \dfrac{2C_{L_H}}{\pi A_H e_H}\overline{q}\overline{S}_H$ $= C_{L_{\delta_H}}\dfrac{2C_{L_H}}{\pi A_H e_H}\overline{q}\overline{S}_H$ Equation (6.32)	$C_{L_{a_H}}\dfrac{2C_{L_H}}{\pi A_H e_H}\overline{q}\overline{S}_H$ Equation (6.33)
Pitching moment, C_m	$C_{M_{AC_w}} + C_{M_{0_F}} + C_{L_{a_w}}(i_w - \alpha_{0_w})\Delta\overline{X}_{AC_{W\&F}}$ $- C_{L_{a_H}}\left(\dfrac{d\varepsilon}{d\alpha}(\alpha_{0_w} - i_w) - \alpha_{0_H}\right)\Delta\overline{X}_{AC_H}\overline{q}\overline{S}_H$ Equation (6.60)	$C_{L_{a_w}}\Delta\overline{X}_{AC_{W\&F}}$ $- C_{L_{a_H}}\overline{\varepsilon}\Delta\overline{X}_{AC_H}\overline{q}\overline{S}_H$ Equation (6.56)	$-C_{L_{a_H}}\alpha_\delta\Delta\overline{X}_{AC_H}\overline{q}\overline{S}_H$ $= -C_{L_{\delta_H}}\Delta\overline{X}_{AC_H}\overline{q}\overline{S}_H$ Equation (6.58)	$-C_{L_{a_H}}\Delta\overline{X}_{AC_H}\overline{q}\overline{S}_H$ Equation (6.59)

Table 6.3 Summary for Vehicle Side Force, Rolling and Yawing Moments, and Drag

Coefficient	Sideslip Angle, β	Rudder Deflection, δ_R	Aileron Deflection, δ_A
Side force, C_S	$C_{S_{\beta_V}}\overline{q}\overline{S}_V$ Equation (6.25)	$C_{S_{\beta_V}}\beta_\delta\overline{q}\overline{S}_V = C_{S_{\delta_V}}\overline{q}\overline{S}_V$ Equation (6.26)	≈ 0
Rolling moment, $C_{L_{Roll}}$	$C_{L_{\beta_w}} + C_{L_{\beta_H}}\overline{q}\overline{S}_H\dfrac{b_H}{b_w} + C_{L_{\beta_V}}\overline{q}\overline{S}_V\dfrac{b_V}{b_w}$ Equation (6.44)	$C_{L_{\delta_V}}\overline{q}\overline{S}_V\dfrac{b_V}{b_w}$ Equation (6.45)	$C_{L_{\delta_{A_{Wing}}}}$ Equation (6.39)
Yawing moment, C_N	$-C_{S_{\beta_V}}\Delta\overline{X}_{AC_V}\overline{q}\overline{S}_V$ Equation (6.68)	$-C_{S_{\delta_V}}\Delta\overline{X}_{AC_V}\overline{q}\overline{S}_V$ Equation (6.69)	$C_{N_{\delta_{A_{Wing}}}}$ Equation (6.65)
Drag, C_D	$\dfrac{2C_{S_V}}{\pi A_V e_V}C_{S_{\beta_V}}\overline{q}\overline{S}_V$ Equation (6.34)	$C_{S_{\beta_V}}\beta_\delta\dfrac{2C_{S_V}}{\pi A_V e_V}\overline{q}\overline{S}_V = C_{S_{\delta_V}}\dfrac{2C_{S_V}}{\pi A_V e_V}\overline{q}\overline{S}_V$ Equation (6.41)	≈ 0

Table 6.5 Dimensional Versus Nondimensional Aerodynamic and Propulsive Moment Derivatives

Partial Derivative ($\bullet = L, M,$ or N)	Dimensional Derivative	Nondimensional Derivative	Nondimensional Parameter
$\dfrac{\partial \bullet_{A \text{ or } P}}{\partial u}\Big\vert_0$	$\left(C_{\bullet_u} + \dfrac{2C_{\bullet_0}}{U_0}\right)q_\infty S_W(\bar{c}_W \text{ or } b_W)$ Equation (6.130) or (6.141)	$(C_{\bullet_{u'}} + 2C_{\bullet_0})q_\infty S_W(\bar{c}_W \text{ or } b_W)$ $C_{\bullet_{u'}} = U_0 C_{\bullet_u}$	$\left(\dfrac{u}{U_0} = u'\right)$
$\dfrac{\partial M_{A \text{ or } P}}{\partial w}\Big\vert_0$	$\dfrac{1}{U_0}C_{M_\alpha}q_\infty S_W \bar{c}_W$ Equation (6.148) or (6.157)	$C_{M_\alpha}q_\infty S_W \bar{c}_W$ $C_{M_\alpha} = U_0 C_{M_w}$	$\left(\dfrac{w}{U_0} = \alpha\right)$
$\dfrac{\partial \bullet_{A \text{ or } P}}{\partial v}\Big\vert_0$	$\dfrac{1}{U_0}(C_{\bullet_\beta} + 2C_{\bullet_0}\beta_0)q_\infty S_W b_W$ Equation (6.164) or (6.173)	$(C_{\bullet_\beta} + 2C_{\bullet_0}\beta_0)q_\infty S_W b_W$ $C_{\bullet_\beta} = U_0 C_{\bullet_v}$	$\left(\dfrac{v}{U_0} = \beta\right)$
$\dfrac{\partial M_{A \text{ or } P}}{\partial q}\Big\vert_0$	$C_{M_q}q_\infty S_W \bar{c}_W$ Equation (6.186) or (6.194)	$C_{M_{q'}}q_\infty S_W \bar{c}_W$ $C_{M_{q'}} = \dfrac{2U_0}{\bar{c}_W}C_{M_q}$	$\left(\dfrac{q\bar{c}_W}{2U_0} = q'\right)$
$\dfrac{\partial L_{A \text{ or } P}}{\partial p}\Big\vert_0$	$C_{L_p}q_\infty S_W b_W$ Equation (6.207) or (6.209)	$C_{L_{p'}}q_\infty S_W b_W$ $C_{L_{p'}} = \dfrac{2U_0}{b_W}C_{L_p}$	$\left(\dfrac{pb_W}{2U_0} = p'\right)$
$\dfrac{\partial N_{A \text{ or } P}}{\partial r}\Big\vert_0$	$C_{N_r}q_\infty S_W b_W$ Equation (6.219) or (6.230)	$C_{N_{r'}}q_\infty S_W b_W$ $C_{N_{r'}} = \dfrac{2U_0}{b_W}C_{N_r}$	$\left(\dfrac{rb_W}{2U_0} = r'\right)$
$\dfrac{\partial L_{A \text{ or } P}}{\partial r}\Big\vert_0$	$C_{L_r}q_\infty S_W b_W$ Equation (6.222) or (6.230)	$C_{L_{r'}}q_\infty S_W b_W$ $C_{L_{r'}} = \dfrac{2U_0}{b_W}C_{L_r}$	$\left(\dfrac{rb_W}{2U_0} = r'\right)$
$\dfrac{\partial M_{A \text{ or } P}}{\partial \dot{\alpha}}\Big\vert_0$	$C_{M_{\dot{\alpha}}}q_\infty S_W \bar{c}_W$ Equation (6.240) or (6.247)	$C_{M_{\dot{\alpha}}}q_\infty S_W \bar{c}_W$ $C_{M_{\dot{\alpha}}} = \dfrac{2U_0}{\bar{c}_W}C_{M_{\dot{\alpha}}}$	$\left(\dfrac{\dot{\alpha}\bar{c}_W}{2U_0} = \dot{\alpha}'\right)$

Table 6.4 Dimensional Versus Nondimensional Aerodynamic and Propulsive Force Derivatives

Partial Derivative ($\bullet$ = X, Y, or Z)	Dimensional Derivative	Nondimensional Derivative	Nondimensional Parameter
$\dfrac{\partial F_{A \text{ or } P_\bullet}}{\partial u}\Big|_0$	$\left(C_{\bullet_u} + \dfrac{2C_{\bullet_0}}{U_0}\right)q_\infty S_W$ Equations (6.122) and (6.133)	$(C_{\bullet_{u'}} + 2C_{\bullet_0})q_\infty S_W$ $C_{\bullet_{u'}} = U_0 C_{\bullet_u}$	$\left(\dfrac{u}{U_0} = u'\right)$
$\dfrac{\partial F_{A \text{ or } P_\bullet}}{\partial w}\Big|_0$	$\dfrac{1}{U_0}C_{\bullet_\alpha}q_\infty S_W$ Equations (6.146) and (6.150)	$C_{\bullet_\alpha}q_\infty S_W$ $C_{\bullet_\alpha} = U_0 C_{\bullet_w}$	$\left(\dfrac{w}{U_0} = \alpha\right)$
$\dfrac{\partial F_{A \text{ or } P_\bullet}}{\partial v}\Big|_0$	$\dfrac{1}{U_0}(C_{\bullet_\beta} + 2C_{\bullet_0}\beta_0)q_\infty S_W$ Equations (6.160) and (6.169)	$(C_{\bullet_\beta} + 2C_{\bullet_0}\beta_0)q_\infty S_W$ $C_{\bullet_\beta} = U_0 C_{\bullet_v}$	$\left(\dfrac{v}{U_0} = \beta\right)$
$\dfrac{\partial F_{A \text{ or } P_\bullet}}{\partial q}\Big|_0$	$C_{\bullet_q}q_\infty S_W$ Equation (6.181) or (6.189)	$C_{\bullet_{q'}}q_\infty S_W$ $C_{\bullet_{q'}} = \dfrac{2U_0}{\bar{c}_W}C_{\bullet_q}$	$\left(\dfrac{q\bar{c}_W}{2U_0} = q'\right)$
$\dfrac{\partial F_{A_Y}}{\partial p}\Big|_0 \left(\dfrac{\partial F_{P_Y}}{\partial p}\Big|_0 \approx 0\right)$	$C_{Y_p}q_\infty S_W$ Equation (6.201)	$C_{Y_{p'}}q_\infty S_W$ $C_{Y_{p'}} = \dfrac{2U_0}{b_W}C_{Y_p}$	$\left(\dfrac{pb_W}{2U_0} = p'\right)$
$\dfrac{\partial F_{A \text{ or } P_\bullet}}{\partial r}\Big|_0$	$C_{\bullet_r}q_\infty S_W$ Equation (6.217) or (6.223)	$C_{\bullet_{r'}}q_\infty S_W$ $C_{\bullet_{r'}} = \dfrac{2U_0}{b_W}C_{\bullet_r}$	$\left(\dfrac{rb_W}{2U_0} = r'\right)$
$\dfrac{\partial F_{A \text{ or } P_\bullet}}{\partial \dot{\alpha}}\Big|_0$	$C_{\bullet_{\dot\alpha}}q_\infty S_W$ Equation (6.238) or (6.245)	$C_{\bullet_{\dot\alpha}}q_\infty S_W$ $C_{\bullet_{\dot\alpha}} = \dfrac{2U_0}{\bar{c}_W}C_{\bullet_{\dot\alpha}}$	$\left(\dfrac{\dot\alpha\bar{c}_W}{2U_0} = \dot\alpha'\right)$

Under this selection of state, response, and input vectors, the four matrices in the state-variable model for the longitudinal dynamics become

$$
A = \begin{bmatrix}
\left(X_u + X_{P_u} + \dfrac{X_{\dot\alpha}(Z_u + Z_{P_u})}{U_0 - Z_{\dot\alpha}} \right) & \left(X_\alpha + \dfrac{X_{\dot\alpha} Z_\alpha}{U_0 - Z_{\dot\alpha}} \right) & -g & \left(X_q + X_{\dot\alpha}\left(\dfrac{U_0 + Z_q}{U_0 - Z_{\dot\alpha}} \right) \right) & 0 \\[3mm]
\left(\dfrac{Z_u + Z_{P_u}}{U_0 - Z_{\dot\alpha}} \right) & \left(\dfrac{Z_\alpha}{U_0 - Z_{\dot\alpha}} \right) & 0 & \left(\dfrac{U_0 + Z_q}{U_0 - Z_{\dot\alpha}} \right) & 0 \\[3mm]
0 & 0 & 0 & 1 & 0 \\[3mm]
\left(M_u + M_{P_u} + \dfrac{M_{\dot\alpha}(Z_u + Z_{P_u})}{U_0 - Z_{\dot\alpha}} \right) & \left(M_\alpha + M_{P_\alpha} + \dfrac{M_{\dot\alpha} Z_\alpha}{U_0 - Z_{\dot\alpha}} \right) & 0 & \left(M_q + M_{\dot\alpha}\left(\dfrac{U_0 + Z_q}{U_0 - Z_{\dot\alpha}} \right) \right) & 0 \\[3mm]
0 & -U_0 & U_0 & 0 & 0
\end{bmatrix}
$$

$$
B = \begin{bmatrix}
\left(X_{\delta_E} + \dfrac{X_{\dot\alpha} Z_{\delta_E}}{U_0 - Z_{\dot\alpha}} \right) & \left(X_T + \dfrac{X_{\dot\alpha} Z_T}{U_0 - Z_{\dot\alpha}} \right) \\[3mm]
\left(\dfrac{Z_{\delta_E}}{U_0 - Z_{\dot\alpha}} \right) & \left(\dfrac{Z_T}{U_0 - Z_{\dot\alpha}} \right) \\[3mm]
0 & 0 \\[3mm]
\left(M_{\delta_E} + \dfrac{M_{\dot\alpha} Z_{\delta_E}}{U_0 - Z_{\dot\alpha}} \right) & \left(M_T + \dfrac{M_{\dot\alpha} Z_T}{U_0 - Z_{\dot\alpha}} \right) \\[3mm]
0 & 0
\end{bmatrix}, \quad
C = \begin{bmatrix}
1 & 0 & 0 & 0 & 0 \\
0 & 1 & 0 & 0 & 0 \\
0 & 0 & 1 & 0 & 0 \\
0 & 0 & 0 & 1 & 0 \\
0 & 0 & 0 & 0 & 1
\end{bmatrix}, \quad
D = \begin{bmatrix}
0 & 0 \\
0 & 0 \\
0 & 0 \\
0 & 0 \\
0 & 0
\end{bmatrix}
$$

$$(8.36)$$

Appendix D

```matlab
% Longitudinal System Definition

A_long = [-0.13653, 12.696, -32.2, 0, 0;

          -0.0042, -3.0366, 0, 1, 0;

          0, 0, 0, 1, 0;

          0.00315, -13.916, 0, -7.68925, 0;

          0, -352, 352, 0, 0];

B_long = [0, 0.0234;

          -0.48, 0;

          0, 0;

          -16.5435, 0;

          0, 0];

C_long = eye(5);

D_long = zeros(5, 2);


sysLong = ss(A_long, B_long, C_long, D_long);

colong = ctrb(A_long, B_long);

conlong = rank(colong);


Kq = .1; % Longitudinal altitude 2 second doublet

ALongAug = A_long + B_long(:,1)*Kq*C_long(4,:);

sysAugLong = ss(ALongAug, B_long, C_long, D_long);

act = tf(-.1, [1 1]);

sysAugLong = series(act, sysAugLong);


% Root Locus and Impulse Response for Longitudinal System

figure(3)

rlocus(sysLong(3,1), sysAugLong(3,1));

legend("original","improved");


figure(4)

impulse(sysLong(3,1), sysAugLong(3,1), 30);
```

```matlab
legend("original","improved");


% Lateral System Definition

A_lat = [-0.07568, 0.275, 0, -1, 0;

         0, 0, 1, 0, 0;

         -23.973, 0, -10.0824, 3.2895, 0;

         8.99, 0, -0.3498, -0.6084, 0;

         0, 0, 0, 1, 0];

B_lat = [0, 0.08465;

         0, 0;

         34.7808, 3.0576;

         -0.4436, -9.194;

         0, 0];

C_lat = eye(5);

D_lat = zeros(5, 2);


sysLat = ss(A_lat, B_lat, C_lat, D_lat);

colat = ctrb(A_lat, B_lat);

conlat = rank(colat);


Kr = 9; % Lateral Roll Rate Gain

ALatAug = A_lat + B_lat(:,2)*Kr*C_lat(4,:);

sysAugLat = ss(ALatAug, B_lat, C_lat, D_lat);


% Root Locus and Impulse Response for Lateral System

figure(5)

rlocus(sysLat(2,2), sysAugLat(2,2));

legend("original","improved");


figure(6)

impulse(sysLat(4,2), sysAugLat(4,2), 30);

legend("original","improved");
```

```matlab
% Simulation Setup

t = 0:0.01:10; % Time vector

u_lat = zeros(length(t), 2);

u_lat(t >= 1 & t <= 2, 1) = 1; % Example: Aileron deflection

x0 = zeros(5,1); % Initial state vector

k = 1; % Scaling factor


% Lateral System Response Simulation

figure(7);

sgtitle('1 second aileron input (with Gain Input)');

y = lsim(sysAugLat, u_lat, t, x0);

subplot(3,2,1)

plot(t, 57.3 * u_lat(:,1))

grid

xlabel('Time, t (sec)')

ylabel('Aileron, deltaA (deg)')

title('Input Aileron Deflection Time History')

subplot(3,2,2);

plot(t, k * y(:,1))

grid

xlabel('Time, t (sec)')

ylabel('Sideslip, beta (deg)')

title('Sideslip Time History')

subplot(3,2,3)

plot(t, k * y(:,2))

grid

xlabel('Time, t (sec)')

ylabel('Bank Angle, phi (deg)')

title('Bank Angle Time History')

subplot(3,2,4)

plot(t, k * y(:,3))

grid

xlabel('Time, t (sec)')
```

```matlab
ylabel('Roll Rate, p (deg/sec)')

title('Roll Rate Time History')

subplot(3,2,5)

plot(t, k * y(:,4))

grid

xlabel('Time, t (sec)')

ylabel('Yaw Rate, q (deg/sec)')

title('Yaw Rate Time History')

subplot(3,2,6)

plot(t, k * y(:,5))

grid

xlabel('Time, t (sec)')

ylabel('Heading, psi (deg)')

title('Heading Time History')


% Longitudinal System Transfer Functions

TFLong = tf(sysLong) % Transfer function of the original longitudinal system

TFAugLong = tf(sysAugLong) % Transfer function of the augmented longitudinal
system


% Lateral System Transfer Functions

TFLat = tf(sysLat); % Transfer function of the original lateral system

TFAugLat = tf(sysAugLat); % Transfer function of the augmented lateral system


% Display Transfer Functions

disp('Original Longitudinal System Transfer Functions:');

disp(TFLong);

disp('Augmented Longitudinal System Transfer Functions:');

disp(TFAugLong);

disp('Original Lateral System Transfer Functions:');

disp(TFLat);

disp('Augmented Lateral System Transfer Functions:');

disp(TFAugLat);
```

Appendix E

Autopilot Matlab Code

```matlab
%% Part 3: Design of Autopilots
% Define constants
U0 =200;


%% Autopilot for Altitude Hold
% Get zero-pole-gain data from augmented system outputs
[z1, p1, k1] = zpkdata(sysAugLong(2,1), 'v');
[z2, p2, k2] = zpkdata(sysAugLong(3,1), 'v');


% Control system design
gammatheta = 1 - zpk(z1, z2, k1/k2);
hgamma = tf(U0, [1 0]);
pi = tf([1 0.32], [1 0]);
lc = tf([1 0.2], [1 1]);
Kh = 0.01;
sys = series(Kh * pi * lc * gammatheta, hgamma);


% Convert to state-space
[A, B, C, D] = ssdata(sys);
Acl = A - B * 1 * C;
sysclalt = ss(Acl, B, C, D);


% Step response
figure(9);
opt = stepDataOptions('StepAmplitude', 100);
step(sysclalt, opt);
title('Altitude Hold Step Response');
```

```matlab
% Bode plot

figure(10);

bode(sysclalt);

title('Altitude Hold Bode Plot');
```

Heading Hold

```matlab
%% Part 3: Design of Autopilots

% Define constants

U0 = 200;

%% Autopilot for Heading Hold

% Get zero-pole-gain data from augmented system outputs

% Assuming sysAugLat is the lateral augmented system matrix

[z1, p1, k1] = zpkdata(sysAugLat(2,1), 'v');

[z2, p2, k2] = zpkdata(sysAugLat(3,1), 'v');


%% Define transfer functions properly

Kh = 0.15; % Gain

leadCompensator = tf([1, 0.5], [1, 2]); % Lead compensator

lagCompensator = tf([1, 0.05], [1, 0.25]);  % Lag compensator

filter = tf([1], [1, 30]);  % Low-pass filter


%% Correct way to apply gain and combine systems in series

% First, apply the gain to one of the transfer functions or create a gain system

gainSystem = tf([Kh], [1]); % Create a transfer function for the gain


% Combine systems in series properly

controlSystem    =    series(series(series(gainSystem,    leadCompensator), lagCompensator), filter);

sysHeading = series(controlSystem, hgamma); % Combine with high-gain element
```

```matlab
% Convert to state-space

[A, B, C, D] = ssdata(sysHeading);

Acl = A - B * 1 * C;

sysclHeading = ss(Acl, B, C, D);


% Step response for a heading change of 3 degrees

figure(11);

opt = stepDataOptions('StepAmplitude', 3); % Set step amplitude to 3 degrees

timeVector = linspace(0, 300, 10000);

step(sysclHeading, timeVector, opt);

title('Heading Hold Step Response: Degrees vs Time');

xlabel('Time (seconds)');

ylabel('Heading Change (degrees)');

ylim([0 4]); % Setting y-axis limits to show from 0 to 4 degrees


% Bode plot for heading control system

figure(12);

bode(sysHeading);

title('Bode Plot for Heading Control System');

xlabel('Frequency (rad/s)');

ylabel('Magnitude (dB) and Phase (degrees)');
```

Appendix G

Flex body code

```matlab
%% Rigid Body Simulation with Updated A and B matrices
A_rigid = [-0.13653, 12.696, -32.2, 0, 0;

           -0.0042, -3.0366, 0, 1, 0;

           0, 0, 0, 1, 0;

           0.00315, -13.916, 0, -7.68925, 0;

           0, -352, 352, 0, 0];
B_rigid = [0, 0.0234;

           -0.48, 0;

           0, 0;

           -16.5435, 0;

           0, 0];
C_rigid = eye(5);
D_rigid = zeros(5,2);


sys_rigid = ss(A_rigid, B_rigid, C_rigid, D_rigid);


t = 0:0.05:10;
u = zeros(2, length(t));  % Initializing input matrix with two inputs
u(1,1:40) = -1/57.3;
u(1,41:80) = 1/57.3;


y_rigid = lsim(sys_rigid, u', t);
y_rigid = y_rigid';


%% Flex Body Simulation with Updated A and B matrices
A_flex = [-0.13653, 12.696, -32.2, 0, 0, 0, 0;

          -0.0042, -3.0366, 0, 1, 0, -0.00634, -0.000340;

          0, 0, 0, 1, 0, 0, 0;

          0.00315, -13.916, 0, -7.68925, 0, -0.1003, -0.560;

          0, -352, 352, 0, 0, 0, 0;
```

```matlab
              0, 0, 0, 0, 0, 0, 1;

              0, 0, 0, 0, 0, -225.3, -1.342];

B_flex = [0, 0.0234;

          -0.48, 0;

          0, 0;

          -16.5435, 0;

          0, 0;

          0, 0;

          -564, 0];

C_flex = eye(7);

D_flex = zeros(7,2);


sys_flex = ss(A_flex, B_flex, C_flex, D_flex);


y_flex = lsim(sys_flex, u', t);

y_flex = y_flex';


%% Plotting Rigid Body Simulation Results

figure(1)

subplot(3,2,1)

plot(t, 57.3*u(1,:))

grid

xlabel('Time, t (sec)')

ylabel('Elevator Angle, deltaE (deg)')

title('Input Elevator Deflection Time History')


subplot(3,2,2);

plot(t, y_rigid(1,:))

grid

xlabel('Time, t (sec)')

ylabel('Surge Velocity, u (fps)')

title('Surge Velocity Time History')
```

```matlab
subplot(3,2,3)

plot(t, 57.3*y_rigid(2,:))

grid

xlabel('Time, t (sec)')

ylabel('Angle of Attack, alpha (deg)')

title('Angle of Attack Time History')


subplot(3,2,4)

plot(t, 57.3*y_rigid(3,:))

grid

xlabel('Time, t (sec)')

ylabel('Attitude Angle, theta (deg)')

title('Attitude Angle Time History')


subplot(3,2,5)

plot(t, 57.3*y_rigid(4,:))

grid

xlabel('Time, t (sec)')

ylabel('Pitch Rate, q (deg/sec)')

title('Rigid Body Pitch Rate History')


subplot(3,2,6)

plot(t, y_rigid(5,:))

grid

xlabel('Time, t (sec)')

ylabel('Altitude, h (ft)')

title('Altitude Time History')


%% Plotting Flex Body Simulation Results

figure(2)

subplot(4,2,1)

plot(t, 57.3*u(1,:))

grid
```

```
xlabel('Time, t (sec)')

ylabel('Elevator Angle, deltaE (deg)')

title('Input Elevator Deflection Time History')


subplot(4,2,2);

plot(t, y_flex(1,:))

grid

xlabel('Time, t (sec)')

ylabel('Surge Velocity, u (fps)')

title('Surge Velocity Time History')


subplot(4,2,3)

plot(t, 57.3*y_flex(2,:))

grid

xlabel('Time, t (sec)')

ylabel('Angle of Attack, alpha (deg)')

title('Angle of Attack Time History')


subplot(4,2,4)

plot(t, 57.3*y_flex(3,:))

grid

xlabel('Time, t (sec)')

ylabel('Attitude Angle, theta (deg)')

title('Attitude Angle Time History')


subplot(4,2,5)

plot(t, 57.3*y_flex(4,:))

grid

xlabel('Time, t (sec)')

ylabel('Pitch Rate, q (deg/sec)')

title('Flex Body Pitch Rate History')


subplot(4,2,6)
```

```
plot(t, y_flex(5,:))

grid

xlabel('Time, t (sec)')

ylabel('Altitude, h (ft)')

title('Altitude Time History')


subplot(4,2,7)

plot(t, y_flex(6,:))

grid

xlabel('Time, t (sec)')

ylabel('Displacement, eta')

title('Mode 1 Displacement')


subplot(4,2,8)

plot(t, y_flex(7,:))

grid

xlabel('Time, t (sec)')

ylabel('Velocity, etadot')

title('Mode 1 Velocity')
```

Pitch with and without feedback

```matlab
% System matrices already defined
A = [-0.13653, 12.696, -32.2, 0, 0, 0, 0;
    -0.0042, -3.0366, 0, 1, 0, -0.00634, -0.000340;
    0, 0, 0, 1, 0, 0, 0;
    0.00315, -13.916, 0, -7.68925, 0, -0.1003, -0.560;
    0, -352, 352, 0, 0, 0, 0;
    0, 0, 0, 0, 0, 0, 1;
    0, 0, 0, 0, 0, -225.3, -1.342];
B = [0, 0.0234;
    -0.48, 0;
    0, 0;
    -16.5435, 0;
    0, 0;
    0, 0;
    -564, 0];


Q = diag([1, 1, 1, 1, 1, 1000, 100]);  % State weighting
R = diag([1, 1]);  % Control input weighting


% Designing the LQR controller
K = lqr(A, B, Q, R);


% Closed-loop system using state-space representation
sys_cl = ss(A - B*K, B, eye(7), zeros(7,2));


% Open-loop system for comparison
sys_ol = ss(A, B, eye(7), zeros(7,2));


t = 0:0.01:10;  % Time vector for simulation
```

```matlab
X0 = [0; 0; 0; 0; 0; 0.01; 0];  % Initial condition


% Zero input for both control channels

u = zeros(2, length(t));


% Simulating the closed-loop response

[Y_cl, T_cl, X_cl] = lsim(sys_cl, u', t, X0);


% Simulating the open-loop response

[Y_ol, T_ol, X_ol] = lsim(sys_ol, u', t, X0);


% Plotting pitch rate comparison

figure;

plot(T_cl, X_cl(:,4), 'b', 'LineWidth', 2); % Closed-loop

hold on;

plot(T_ol, X_ol(:,4), 'r--', 'LineWidth', 2); % Open-loop

xlabel('Time (s)');

ylabel('Pitch Rate, q (rad/s)');

title('Comparison of Pitch Rate With and Without Feedback Control');

legend('With Feedback', 'Without Feedback');

grid on;
```